JOC Article
pubs.acs.org/joc

Very Contracted to Extended *co*-Conformations with or without Oscillations in Two- and Three-Station [c2]Daisy Chains

Camille Romuald, Eric Busseron, and Frédéric Coutrot*

Institut des Biomolécules Max Mousseron (IBMM), UMR 5247CNRS - Universités Montpellier 2 et 1, Bâtiment de recherche Max Mousseron, Ecole Nationale Supérieure de Chimie de Montpellier, 8 rue de l'Ecole Normale, 34296 Montpellier Cedex 5, France

frederic.coutrot@univ-montp2.fr

Received June 30, 2010

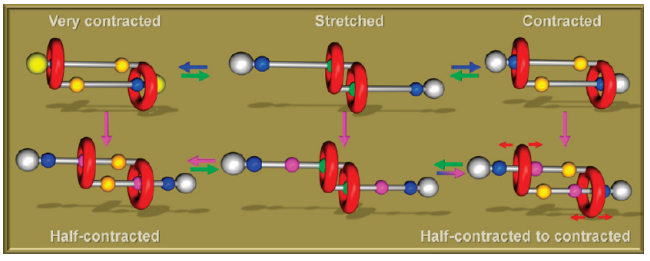

The syntheses of various two- and three-station mannosyl [c2]daisy chains, based on a dibenzo-24-crown-8 macrocyclic moiety and an ammonium, a triazolium, and a mono- or disubstituted pyridinium amide station, are reported. The ability of these molecules to act as molecular machine based mimetics has been further studied by ^{1}H NMR studies. In all the protonated ammonium states, the interwoven rotaxane dimers adopt an extended *co*-conformation. However, carbamoylation of the ammonium station led to many different other [c2]daisy chain *co*-conformations, depending on the other molecular stations belonging to the axle. In the two-station [c2]daisy chains containing an ammonium and a mono- or disubstituted pyridinium amide station, two large-amplitude relative movements of the interwoven components were noticed and afforded either an extended and a contracted or very contracted state with, in the latter case, an impressive chairlike conformational flipping of the mannopyranose from $^1C_4$ to $^4C_1$. In the case of the three-station-based [c2]daisy chains containing an ammonium, a triazolium, and disubstituted pyridinium amide, an extended and a half-contracted molecular state could be obtained because of the stronger affinity of the dibenzo-24-crown-8 part for, respectively, the ammonium, the triazolium, and the disubstituted pyridinium amide. Eventually, with axles comprising an ammonium, a triazolium, and a monosubstituted pyridinium amide, an extended conformation was noticed in the protonated state whereas a continuous oscillation between half-contracted and contracted states, in fast-exchange on the NMR time scale, was triggered by carbamoylation. Variations of the solvent or the temperature allow the modification of the population of each *co*-conformer. Thermodynamic data provided a small free Gibbs energy ΔG of 2.1 kJ·mol^{-1} between the two translational isomers at 298 K.

Introduction

Molecular machines based on rotaxane architectures have attracted much interest during the past decades,[1] especially because the presence and the relative movements of the macrocycle (translation and circumrotation) in the interlocked component have been shown to dramatically modify the properties of the molecule. Many of these molecular

(1) (a) Kay, E. R.; Leigh, D. A.; Zerbetto, F. *Angew. Chem., Int. Ed.* **2007**, *46*, 72–191. (b) Schalley, C. A.; Beizai, K.; Vögtle, F. *Acc. Chem. Res.* **2001**, *34*, 465–476. (c) Balzani, V.; Gomez-Lopez, M.; Stoddart, J. F. *Acc. Chem. Res.* **1998**, *31*, 405–414. (d) Collin, J.- P.; Dietrich-Buchecker, C.; Gavina, P.; Jimenez-Molero, M. C.; Sauvage, J.-P. *Acc. Chem. Res.* **2001**, *34*, 477–487. (e) Balzani, V.; Credi, A.; Venturi, M. *Nanotoday* **2007**, *2*, 18–2. (f) Balzani, V.; Credi, A.; Raymo, F. M.; Stoddart, J. F. *Angew. Chem., Int. Ed.* **2000**, *39*, 3348–3391. (g) Kinbara, K.; Aida, T. *Chem. Rev.* **2005**, *105*, 1377–1400. (h) Griffiths, K. E.; Stoddart, J. F. *Pure Appl. Chem.* **2008**, *80*, 485–506.

(2) For some examples, see: (a) Berna, J.; Leigh, D. A.; Lubomska, M.; Medoza, S. M.; Perez, E. M.; Rudolf, P.; Teobaldi, G.; Zerbetto, F. *Nat. Mater.* **2005**, *4*, 704–710. (b) Li, D.; Paxton, W. F.; Baughman, R. H.; Huang, T. J.; Stoddart, J. F.; Weiss, P. S. *MRS Bull.* **2009**, *34*, 671–681. (c) Juluri, B. K.; Kumar, A. S.; Liu, Y.; Ye, T.; Yang, Y.-W.; Flood, A. H.; Stoddart, J. F.; Weiss, P. S.; Huang, T. J. *ACS Nano* **2009**, *3*, 291–300. (d) Liu, Y.; Flood, A. H.; Bonvallet, P. A.; Vignon, S. A.; Northrop, B.; Tseng, H.-R.; Jeppesen, J.; Huang, T. J.; Brough, B.; Baller, M.; Magonov, S.; Solares, S.; Goddard, W. A., III; Ho, C.-M.; Stoddart, J. F. *J. Am. Chem. Soc.* **2005**, *127*, 9745–9759.

Published on Web 09/03/2010 DOI: 10.1021/jo101234u

machines have been devoted to nanotechnology in the domain of materials,[2] whereas the potential interest of rotaxane-based molecules in the medicinal field has just emerged in the past few years as a promising and exciting investigation field.[3] As a part of rotaxane molecular machines, [c2]daisy chains[4] acting as molecular muscles[5] represent interesting targets, but few synthetic examples have been reported so far. [c2]Daisy chains consist of a rotaxane dimer, in which each interwoven hermaphrodite monomer contains a macrocycle linked to a thread, which includes one or more template moieties for the macrocycle. When two molecular stations are located in the thread, such molecules can adopt either a stable contracted or a stretched *co*-conformation, depending on the relative affinity of the two sites of recognition for the macrocycle. The incorporation of [c2]daisy chain moieties in polymeric chains has been recently realized by Stoddart and Grubbs in order to modify the length of polymers by controlling the pH, hence to change material properties.[6] To the best of our knowledge, no molecular muscle, including more than two stations, and which could then adopt more than two *co*-conformations has been envisaged until now. Moreover, no molecular muscles have been designed up to date to possess either a stretched *co*-conformation or a continuous oscillating shuttling behavior between a contracted and a half-contracted *co*-conformation as in a degenerate-like [2]rotaxane molecular machine.[7] We have recently described a very direct and efficient access to bistable pH-sensitive mannosyl molecular machines[8] and molecular muscle[9] containing a dibenzo-24-crown-8 (DB24C8) ring or a derivative and based on an ammonium and either a pyridinium amide or a triazolium molecular stations. Here, we report on the synthesis and the shuttling behavior of different [c2]daisy chains, consisting of mannosyl ends and DB24C8-like rings and based on two or three molecular stations (ammonium, triazolium, pyridinium amide stations) for the DB24C8 ring derivatives. In the case of the three-station-containing [c2]daisy chains, each molecular station was spaced out by a hexamethylenic alkyl chain, allowing very well differentiated *co*-conformations of the molecules (Figure 1). For all of the considered interwoven [c2]daisy chain structures, the protonated ammonium state **1**−**2** allows for a stretched *co*-conformation in which the two mannosyl ends are located far away from each other. Since deprotonation of encircled ammonium required strong bases for most of our interwoven molecules, and since the free nucleophilic amine-containing molecular muscle was not stable enough in time, it often led to side degradation. To displace the protonation/deprotonation equilibrium, a mild carbamoylation of the generated amine using a weak base was used instead and afforded different desired unstretched

(3) (a) Fernandes, A.; Viterisi, A.; Coutrot, F.; Potok, S.; Leigh, D. A.; Aucagne, V.; Papot, S. *Angew. Chem., Int. Ed.* **2009**, *48*, 6443–6447. (b) Nguyen, T. D.; Tseng, H. R.; Celestre, P. C.; Flood, A. H.; Liu, Y.; Stoddart, J. F.; Zink, J. I. *Proc. Natl. Acad. Sci. U.S.A.* **2005**, *102*, 10029–10034. (c) Leung, K. C. F.; Nguyen, T. D.; Stoddart, J. F.; Zink, J. I. *Chem. Mater.* **2006**, *18*, 5919–5928. (d) Nguyen, T. D.; Leung, K. C. F.; Liong, M.; Pentecost, J. F.; Stoddart, J. F.; Zink, J. I. *Org. Lett.* **2006**, *8*, 3363–3366. (e) Nguyen, T. D.; Liu, Y.; Saha, S.; Leung, K. C. F.; Stoddart, J. F.; Zink, J. I. *J. Am. Chem. Soc.* **2007**, *129*, 626–634. (f) Nguyen, T. D.; Leung, K. C. F.; Liu, Y.; Stoddart, J. F.; Zink, J. I. *Adv. Funct. Mater.* **2007**, *17*, 2101–2110. (g) Angelo, S.; Johansson, E.; Stoddart, J. F.; Zink, J. I. *Adv. Funct. Mater.* **2007**, *17*, 2261–2271. (h) Patel, K.; Angelo, S.; Dichtel, W. R.; Coskun, A.; Yang, Y. W.; Zink, J. I.; Stoddart, J. F. *J. Am. Chem. Soc.* **2008**, *130*, 2382–2383. (i) Agelos, S.; Yang, Y. W.; Patel, K.; Stoddart, J. F.; Zink, J. *Angew. Chem., Int. Ed.* **2008**, *47*, 2222–2226. (j) Klichko, Y.; Liong, M.; Choi, E.; Angelo, S.; Nel, A. E.; Stoddart, J. F.; Tamanoi, F.; Zink, J. I. *J. Am. Ceram. Soc.* **2009**, *92*, S2–S10. (k) Ferris, D. P.; Zhao, Y. L.; Khashab, N. M.; Khatib, H. A.; Stoddart, J. F.; Zink, J. *J. Am. Chem. Soc.* **2009**, *131*, 1686–1688. (l) Khashab, N. M.; Trabolsi, A.; Lau, Y. A.; Ambrogio, M. W.; Friedman, D. C.; Khatib, H. A.; Zink, J. I.; Stoddart, J. F. *Eur. J. Org. Chem.* **2009**, 1669–1673. (m) Khashab, N. M.; Belowich, M. E.; Trabolsi, A.; Friedman, D. C.; Valente, C.; Lau, Y. N.; Khatib, H. A.; Zink, J. I.; Stoddart, J. F. *Chem. Commun.* **2009**, 5371–5373. (n) Liong, M.; Angelo, S.; Choi, E.; Patel, K.; Stoddart, J. F.; Zink, J. I. *J. Mater. Chem.* **2009**, *19*, 6251–6257. (o) Angelos, S.; Yang, Y. W.; Khashab, N. M.; Stoddart, J. F.; Zink, J. I. *J. Am. Chem. Soc.* **2009**, *131*, 11344–11346. (p) Angelo, S.; Khashab, N. M.; Yang, Y. W.; Trabolsi, A.; Khatib, H. A.; Stoddart, J. F.; Zink, J. I. *J. Am. Chem. Soc.* **2009**, *131*, 12912–12914. (q) Du, L.; Liao, S. J.; Khatib, H. A.; Stoddart, J. F.; Zink, J. I. *J. Am. Chem. Soc.* **2009**, *131*, 15136–15142. (r) Wang, X.; Bao, X.; Mc Farland-Mancini, M.; Isaacsohn, I.; Drew, A. F.; Smithrud, D. B. *J. Am. Chem. Soc.* **2007**, *129*, 7284–7293. (s) Bao, X.; Isaacsohn, I.; Drew, A. F.; Smithrud, D. B. *J. Am. Chem. Soc.* **2006**, *128*, 12229–12238. (t) Smukste, I.; Smithrud, D. B. *J. Org. Chem.* **2003**, *68*, 2547–2558. (u) Dvornikovs, V.; House, B. E.; Kaetzel, M.; Dedman, J. R.; Smithrud, D. B. *J. Am. Chem. Soc.* **2003**, *125*, 8290–8301. (v) Zhu, J.; House, B. E.; Fleck, E.; Isaacsohn, I.; Drew, A. F.; Smithrud, D. B. *Bioorg. Med. Chem. Lett.* **2007**, *17*, 5058–5062. (w) Zhu, J.; Mc Farland-Mancini, M.; Drew, A. F.; Smithrud, D. B. *Bioorg. Med. Chem. Lett.* **2009**, *19*, 520–523. (x) Eguchi, M.; Ooya, T.; Yui, N. *J. Controlled Release* **2004**, *96*, 301–307. (y) Ooya, T.; Arizono, K.; Yui, N. *Polym. Adv. Technol.* **2000**, *11*, 642–651. (z) Ooya, T.; Yui, N. *J. Controlled Release* **1999**, *58*, 251–269. (aa) Ooya, T.; Yui, N. *Crit. Rev. Ther. Drug* **1999**, *16*, 289–330. (ab) Ooya, T.; Yui, N. *STP Pharma Sci.* **1999**, *9*, 129–138. (ab) Ooya, T.; Yui, N. In *Biomedical Polymers and Polymer Therapeutics*; Kluwer Academic/Plenum Publishers: New York, 2001; pp 75−90. (ac) Cheetham, A. G.; Hutchings, M. G.; Claridge, T. D. W.; Anderson, H. L. *Angew. Chem., Int. Ed.* **2006**, *45*, 1596–1599. (ad) Katz, E.; Sheeney-Haj-Ichia, L.; Willner, I. *Angew. Chem., Int. Ed.* **2004**, *43*, 3292–3300. (ae) Belitsky, J. M.; Nelson, A.; Stoddart, J. F. *Org. Biomol. Chem.* **2006**, *4*, 250–256. (af) Nelson, A.; Belitsky, J. M.; Vodal, S.; Joiner, C. S.; Baum, L. G.; Stoddart, J. F. *J. Am. Chem. Soc.* **2004**, *126*, 11914–11922. (ag) Chwalek, M.; Auzély, R.; Fort, S. *Org. Biomol. Chem* **2009**, *7*, 1680–1688. (ah) Yui, N.; Ooya, T. *Chem.—Eur. J.* **2006**, *12*, 6730–6737. (ah) Ooya, T.; Eguchi, M.; Yui, N. *J. Am. Chem. Soc.* **2003**, *125*, 13016–13017.

(4) (a) Cantrill, S. J.; Youn, G. J.; Stoddart, J. F. *J. Org. Chem.* **2001**, *66*, 6857–6872. (b) Chiu, S. H.; Rowan, S. J.; Cantrill, S. J.; Stoddart, J. F.; White, A. J. P.; Williams, D. J. *Chem. Commun.* **2002**, 2948–2949. (c) Amirsakis, D. G.; Elizarov, A. M.; Garcia-Garibay, M. A.; Glink, P. T.; Stoddart, J. F.; White, A. J. P.; Williams, D. J. *Angew. Chem., Int. Ed.* **2003**, *42*, 1126–1132. (d) Fujimoto, T.; Sakata, Y.; Kaneda, T. *Chem. Commun.* **2000**, 2143–2144. (e) Onagi, H.; Easton, C. J.; Lincoln, S. F. *Org. Lett.* **2001**, *3*, 1041–1044. (f) Park, J. W.; Lee, S. Y.; Song, H. J.; Park, K. K. *J. Org. Chem.* **2005**, *70*, 9505–9513. (g) Rowan, S. J.; Cantrill, S. J.; Stoddart, J. F.; White, A. J. P.; Williams, D. J. *Org. Lett.* **2000**, *2*, 759–762. (h) Ueng, S. H.; Hsueh, S. Y.; Lai, C. C.; Liu, Y. H.; Peng, S. M.; Chiu, S. H. *Chem. Commun.* **2008**, 817–819. (i) Yamaguchi, N.; Gibson, H. W. *Chem. Commun.* **1999**, 789–790. (j) Rowan, S. J.; Stoddart, J. F. *Polym. Adv. Technol.* **2002**, *13*, 777–787. (k) Ashton, P. R.; Parsons, I. W.; Raymo, F. M.; Stoddart, J. F.; White, A. J. P.; Williams, D. J.; Wolf, R. *Angew. Chem., Int. Ed.* **1998**, *37*, 1913–1916. (l) Ashton, P. R.; Baxter, I.; Cantrill, S. J.; Fyfe, M. C. T.; Glink, P. T.; Stoddart, J. F.; White, A. J. P.; Williams, D. J. *Angew. Chem., Int. Ed.* **1998**, *37*, 1294–1297.

(5) (a) Bonnet, S.; Collin, J. P.; Koizumi, M.; Mobian, P.; Sauvage, J. P. *Adv. Mater.* **2006**, *18*, 1239–1250. (b) Collin, J. P.; Heitz, V.; Bonnet, S.; Sauvage, J. P. *Inorg. Chem. Commun.* **2005**, *8*, 1063–1074. (c) Jimenez-Molero, M. C.; Dietrich-Buchecker, C.; Sauvage, J. P. *Chem.—Eur. J.* **2002**, *8*, 1456–1466. (d) Colasson, B. X.; Dietrich-Buchecker, C.; Jimenez-Molero, M. C.; Sauvage, J. P. *J. Phys. Org. Chem.* **2002**, *15*, 476–483. (e) Collin, J. P.; Dietrich-Buchecker, C.; Gavina, P.; Jimenez-Molero, M. C.; Sauvage, J. P. *Acc. Chem. Res.* **2001**, *34*, 477–487. (f) Consuelo Jimenez, M.; Dietrich-Buchecker, C.; Sauvage, J. P. *Angew. Chem., Int. Ed.* **2000**, *39*, 3284–3287. (g) Wu, J.; Leung, K. C. F.; Benitez, D.; Han, J. Y.; Cantrill, S. J.; Fang, L.; Stoddart, J. F. *Angew. Chem., Int. Ed.* **2008**, *47*, 7470–7474. (h) Dawson, R. E.; Lincoln, S. F.; Easton, C. J. *Chem. Commun.* **2008**, 3980–3982.

(6) (a) Fang, L.; Hmadeh, M.; Wu, J.; Olson, M. A.; Spruell, J. M.; Trabolsi, A.; Yang, Y.-W.; Elhabiri, M.; Albrecht-Gary, A.-M.; Stoddart, J. F. *J. Am. Chem. Soc.* **2009**, *131*, 7126–7134. (b) Clark, P. G.; Day, M. W.; Grubbs, R. H. *J. Am. Chem. Soc.* **2009**, *131*, 13631–13633. (c) Guidry, E. N.; Li., J.; Stoddart, J. F.; Grubbs, R. H. *J. Am. Chem. Soc.* **2007**, *129*, 8944–8945.

(7) (a) Yoon, I.; Benitez, D.; Zhao, Y.-L.; Miljanic, O. S.; Kim, S. −Y.; Tkatchouk, E.; Leung, K. C.-F.; Khan, S. I.; Goddard, W. A., III; Stoddart, J. F. *Chem.—Eur. J.* **2009**, *15*, 1115–1122. (b) Credi, A. *J. Phys.: Condens. Matter.* **2006**, *18*, 1779–1795. (c) Anelli, P. L.; Spencer, N.; Stoddart, J. F. *J. Am. Chem. Soc.* **1991**, *113*, 5131–5133. (d) Balzani, V.; Credi, A.; Ferrer, B.; Silvi, S.; Venturi, M. *Top. Curr. Chem.* **2005**, *262*, 1–27.

(8) (a) Coutrot, F.; Busseron, E. *Chem.—Eur. J.* **2008**, *14*, 4784–4787. (b) Coutrot, F.; Busseron, E. *Chem.—Eur. J.* **2009**, *15*, 5186–5190.

(9) Coutrot, F.; Romuald, C.; Busseron, E. *Org. Lett.* **2008**, *10*, 3741–3744.

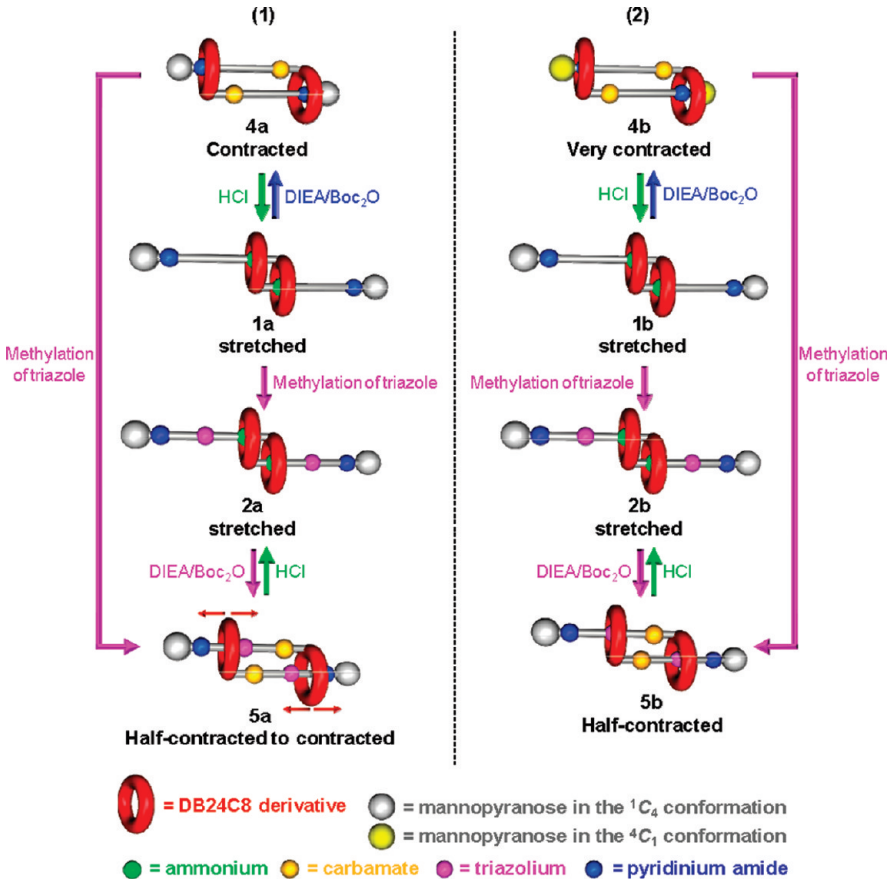

FIGURE 1. Cartoon representation of the different *co*-conformational states adopted by the mannosyl [c2]daisy chains **1**−**5** in (1) the monosubstituted pyridinium amide station series **a** and (2) the disubstituted pyridinium amide series **b**.

compounds in a cleaner manner. When only two different molecular stations are present on the axles (compounds **4a**,**b** containing an ammonium and either a mono- or a disubstituted pyridinium amide stations), large-amplitude molecular shuttlings toward a contracted or a very contracted state can be observed after the deprotonation and the further carbamoylation of the amine, depending on the substitution of the pyridinium amide. In the unique case of the very contracted *co*-conformation, the displacement of the DB24C8 rings around the pyridinium triggers a dramatic switch of the chairlike conformation of the mannopyranose. If three stations are incorporated in the axle (compounds **5a**,**b** including ammonium, triazolium, and mono- or disubstituted pyridinium amide stations), the shuttling of the system after deprotonation/carbamoylation is quite different and depends on the different relative affinity of both the triazolium and the mono- or disubstituted pyridinium amide for the DB24C8 moiety. Whereas in the presence of the disubstituted pyridinium amide station the [c2]daisy chain **5b** can only adopt a half-contracted state, the machine acts very differently with the monosubstituted pyridinium amide. Effectively, after deprotonation/carbamoylation of the best ammonium station, the two DB24C8 macrocycles shuttle toward both the triazolium and the pyridinium amide moieties. Since these two stations have almost similar affinity at room temperature for the DB24C8, a novel oscillating molecular muscle, in which a contracted and a half-contracted *co*-conformation are in fast equilibrium, is obtained. This oscillation of the macrocycles can be stopped by decarbamoylation/protonation or by decreasing the temperature. More interestingly, the *ratio* at room temperature between the two translational isomers (i.e., between the contracted and the half-contracted *co*-conformation), which are in fast exchange on the NMR time scale, strongly depends on both the temperature and the nature of the solvent.

Results and Discussion

1. Synthesis of the Stretched Mannosyl [c2]Daisy Chains 1a, b and 2a,b Containing Respectively Two and Three Molecular Stations. The strategy used to obtain the interwoven molecules **1** was based on an end-capping using the copper(I)-catalyzed Huisgen[10] alkyne−azide 1,3-dipolar cycloaddition, also called "the CuAAC click chemistry"[11] (Scheme 1) between the azido pyridinium mannosides **6a** or **6b** (1 equiv) and the terminal alkyne pseudo[c2]daisy chain **7** (1 equiv) in the presence of a catalytic amount of 2,6-lutidine (0.1 equiv) and $Cu(CH_3CN)_4PF_6$ (1 equiv).[12] Interwoven mannosyl[c2]daisy chains **1a** and **1b** were isolated in, respectively, 77% and 74% yield after silica gel chromatographic column purification. Interestingly, no other interlocked structure was isolated, which demonstrates the much higher affinity of the DB24C8 cavity for the ammonium template than for the mono- or disubstituted pyridinium amide one. The regioselective *N*-methylation of the triazole **1a** and **1b** was further carried out using iodomethane as reactant and solvent at room temperature, and the triazolium iodide, which was obtained after evaporation, was

SCHEME 1. Synthesis of the Stretched [c2]Daisy Chains 1a,b and 2a,b Containing, Respectively, Two or Three Molecular Stations

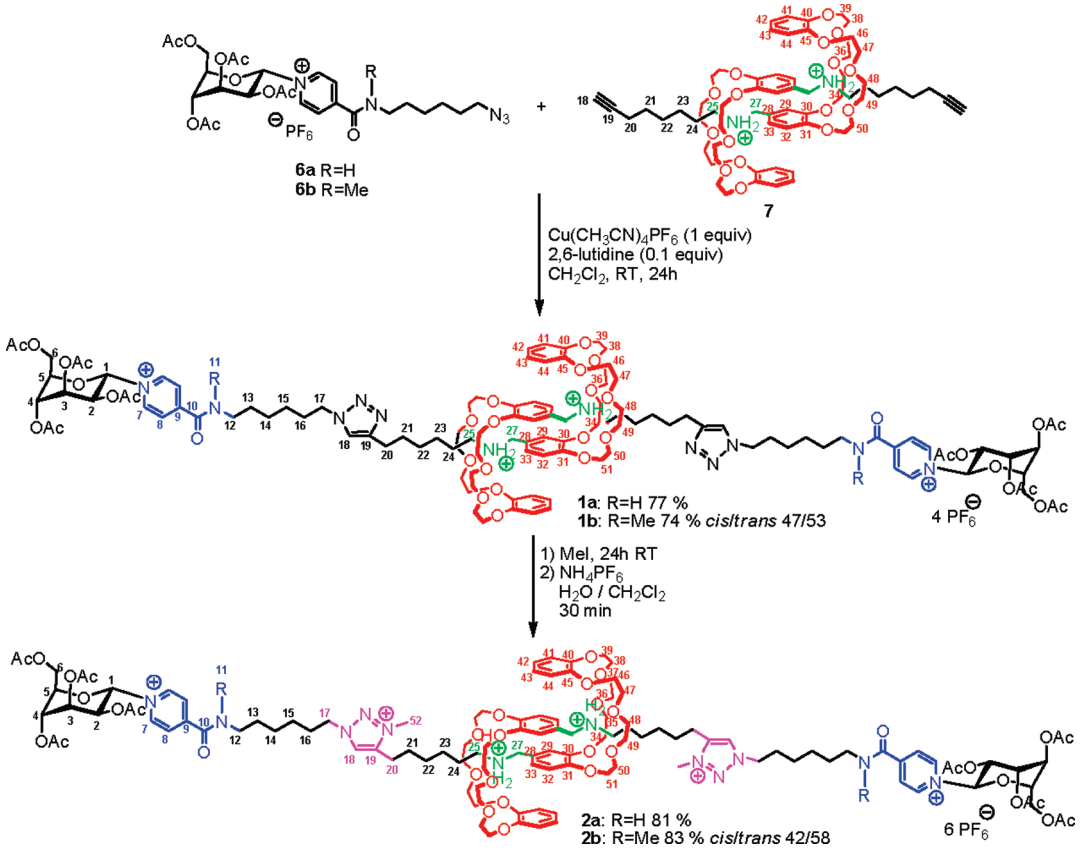

then submitted to an anion-exchange using ammonium hexafluorophosphate. The mannosyl [c2]daisy chains **2a**,**b** containing three molecular stations for the DB24C8 ring derivative were obtained in, respectively, 81% and 83% yield (Scheme 1).

2. Molecular Machinery on Rotaxane Dimers 1a,b and 2a,b Containing, Respectively, Two and Three Molecular Stations. 2.1. Preliminary Attempts of Deprotonation of Rotaxane Dimers 1−2. In a first instance, the deprotonation of the two rotaxane dimers **1a** and **1b** was investigated in order to study the possible pH-sensitive large-amplitude contraction/stretching movements of the molecular muscles. Unfortunately, clean deprotonation of **1a** or **1b** was not possible whatever the bases (DIEA, NaOH, DBU, or P_1-phosphazene) or the solvent used (Scheme 2). On one hand, weak bases were not found to be sufficiently basic to deprotonate the ammonium because of the enhanced pK_a of the ammonium/amine pair when the ammonium moiety is complexed with the oxygens of the DB24C8. This was particularly surprising as we reported in a recent paper the easy deprotonation of ammonium moieties of rotaxane dimer by washing with NaOH.[9] Actually, an important difference between our previous structure and the new ones resides in the absence of a molecular station at a reasonable distance from the ammonium, which, one can assume, helps the deprotonation by assisting the move of the DB24C8. On the other hand, the use of strong bases caused nonelucidated side degradation of the rotaxane dimers. Nevertheless, in the case of the [c2]daisy chain **2a**, in which a triazolium station resides at a reasonable distance from the ammonium site, deprotonation of the ammonium occurred using NaOH and led, at room temperature, to a continuous oscillation of the DB24C8 derivative around both the triazolium and the monosubstituted pyridinium amide (Scheme 2). It is interesting to notice that even though deprotonation of **2a** was

(10) (a) Huisgen, R. *Pure. Appl. Chem.* **1989**, *61*, 613–628. (b) Huisgen, R. *Angew. Chem.* **1963**, *75*, 604−637; *Angew. Chem., Int. Ed. Engl.* **1963**, *2*, 565−598. (c) Huisgen, R.; Szeimies, G.; Möbius, L. *Chem. Ber.* **1967**, *100*, 2494–2507. (d) Huisgen, R. *Angew. Chem.* **1963**, *75*, 742−754; *Angew. Chem., Int. Ed. Engl.* **1963**, *2*, 633−645. For a recent review of the application of copper(I)-catalyzed azide−alkyne 1,3-cycloaddition to catenane and rotaxane synthesis, see: Hänni, K. D.; Leigh, D. A. *Chem. Soc. Rev.* **2010**, *39*, 1240–1251. For recent syntheses of rotaxanes using a copper(I)-catalyzed azide−alkyne 1,3-cycloaddition strategy, see: (e) Aucagne, V.; Hänni, K. D.; Leigh, D. A.; Lusby, P. J.; Walker, D. B. *J. Am. Chem. Soc.* **2006**, *128*, 2186–2187. (f) Mobian, P.; Collin, J. −P.; Sauvage, J. −P. *Tetrahedron Lett.* **2006**, *47*, 4907–4909. (g) Braunschweig, A. B.; Dichtel, W. R.; Miljanic, O. S.; Olson, M. A.; Spruell, J. M.; Khan, S. I.; Heath, J. R.; Stoddart, J. F. *Chem. Asian. J.* **2007**, *2*, 634–647. (h) Aucagne, V.; Berna, J.; Crowley, J. D.; Goldup, S. M.; Hänni, K. D.; Leigh, D. A.; Lusby, P. J.; Ronaldson, V. E.; Slawin, A. M. Z.; Viterisi, A.; Walker, D. B. *J. Am. Chem. Soc.* **2007**, *129*, 11950–11963. (i) Aprahamina, I.; Yasuda, T.; Ikeda, T.; Saha, S.; Dichtel, W. R.; Isoda, K.; Kato, T.; Stoddart, J. F. *Angew. Chem., Int. Ed.* **2007**, *46*, 4675–4679. (j) Aprahamian, I.; Miljanic, O.; Dichtel, W. R.; Isoda, K.; Yasuda, T.; Kato, T.; Stoddart, J. F. *Bull. Chem. Soc. Jpn.* **2007**, *80*, 1856–1859. (k) Aprahamian, I.; Dichtel, W. R.; Ikeda, T.; Heath, J. R.; Stoddart, J. F. *Org. Lett.* **2007**, *9*, 1287–1290. (l) Miljanic, O. S.; Dichtel, W. R.; Aprahamian, I.; Rohde, R. D.; Agnew, H. D.; Heath, J. R.; Stoddart, J. F. *QSAR Comb. Sci.* **2007**, *11*−*12*, 1165–1174. (m) Spruell, J. M.; Dichtel, W. R.; Heath, J. R.; Stoddart, J. F. *Chem.—Eur. J.* **2008**, *14*, 4168–4177. (n) Zhang, W.; Dichtel, W. R.; Stieg, A. Z.; Benitez, D.; Gimzewski, J. K.; Heath, J. R.; Stoddart, J. F. *Proc. Natl. Acad. Sci. U.S.A.* **2008**, *105*, 6514–6519. (o) Zheng, H.; Zhou, W.; Lv, J.; Yin, X.; Li, Y.; Liu, H.; Li, Y. *Chem.—Eur. J.* **2009**, *15*, 13253–13262.

(11) (a) Kolb, H. C.; Finn, M. G.; Sharpless, K. B. *Angew. Chem., Int. Ed.* **2001**, *40*, 2004–2021. (b) Lutz, J. F. *Angew. Chem., Int. Ed.* **2008**, *47*, 2182–2184. (c) Meldal, M.; Tornoe, C. W. *Chem. Rev.* **2008**, *108*, 2952–3015.

(12) Compounds **6** and **7** were previously synthesized according to the experimental procedures described in the Supporting Information.

SCHEME 2. Molecular Machinery Using a pH *Stimulus* on (a) the Mannosyl [c2]Daisy Chains 1a,b and (b) 2a Containing, Respectively, Two and Three Molecular Stations

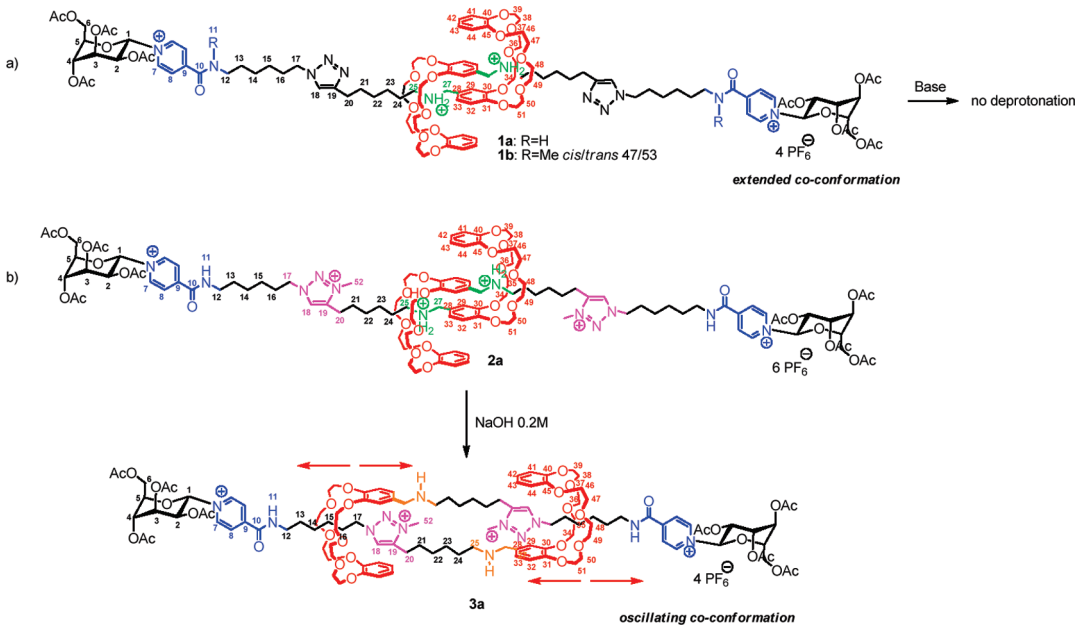

possible, the oscillating molecular muscle **3a** could only be isolated for a short time as it underwent very quick self-degradation.

2.2. Deprotonation−Carbamoylation of Rotaxane Dimers 1−2. To remedy the problem of the tricky deprotonation, which is either impossible in the case of the two station-containing rotaxane dimers or accompanied by side-degradation in the case of the three station-containing rotaxane dimers, we decided to displace the deprotonation equilibrium, under milder conditions, by consuming the in situ generated amine via carbamoylation (Scheme 3).

In a typical procedure, the reaction was carried out in acetonitrile using an excess of the diisopropylethylamine Hünig's base[13] (DIEA, 8 equiv) and di-*tert*-butyl dicarbonate (Boc_2O, 16 equiv). Almost complete conversion took as long as 2.5 to 16 days at room temperature to yield, after Sephadex chromatographic purification, traces to 75% of the desired compounds **4a**,**b** and **5a**,**b**, depending on the presence of the triazolium moiety and on the substitution of the pyridinium amide. As a comparison, the same conditions of deprotonation/carbamoylation were applied to the compound **7**, which is not end-capped: in that case, the reaction could be achieved in as fast as 2 h in a 93% yield after purification. This highlights the very low reactivity of the ammonium molecular station when interlocked in such a stable assembled structure, compared to when it is only incorporated in a pseudo [c2]daisy chain (i.e., without any bulky stoppering ends). It is noteworthy that the formation of **4b** was very slow, probably because the disubstituted pyridinium amide constitutes the weakest molecular station for the DB24C8 part and, hence, does not help sufficiently the deprotonation of the ammonium. For the preparation of **5a**, only traces of desired product were collected; however, **5a** could be very efficiently obtained from **4a** by methylation and exchange of counteranion in an overall excellent yield of 96%. The same synthetic pathway could also be utilized from **4b** to generate **5b** in 91% yield.

The recovery of the starting stretched material **1a**,**b** and **2a**,**b** was realized by standard removal of the Boc protection using a solution of hydrochloric acid in diethyl ether, followed by an exchange of the counteranion.

The chemical *stimuli* applied to our [c2]daisy chains generated various highly controllable *co*-conformations, from a stretched to a very contracted state via half-contracted and contracted states with different behaviors. Whereas one of them, **5a**, undergoes a continuous oscillating state at room temperature, in the case of **4b**, an impressive conformational flipping of the mannopyranosyl ring extremities from $^1C_4$ to $^4C_1$ was noticed. All these different *co*-conformations, which actually result from the different affinities of the molecular stations for the DB24C8 derivative, were established by the following ^{1}H NMR studies.

a. Molecular Machinery of the Molecular Muscle Mimic System 1a/4a. The comparison of ^{1}H NMR spectra of mannosyl [c2]daisy chains **1a** and **4a** with their uncomplexed monomer analogues **1au** and **4au** reveals the interlocked [c2]daisy chain architecture and the localization of the DB24C8 along the threaded axle in **1a** and **4a**, thus demonstrating the stretched and the contracted *co*-conformations indicated in Scheme 3 (Figure 2a,b). Indeed, in the rotaxane dimer **1a**, the same ^{1}H NMR observations as those recently reported for the interwoven structure evidence of pseudorotaxane dimer **7**[9] were noticed for the hydrogens of the DB24C8 part. The methylenic hydrogens of the DB24C8 are split in the interwoven rotaxane dimer **1a**, since they are facing the two nonsymmetrical extremities of the molecule, and the hydrogens of the aromatic rings of the DB24C8, H_{29-32}, and H_{41-44}, are all shielded, indicating a "sandwich"-like *co*-conformation. This *co*-conformation is confirmed by the absence of significant variations of the H_{20-24} which are next to the interaction site and which are not undergoing any shielding effect by the aromatic ring of the

(13) Hünig, S.; Kiessel, M. *Chem. Ber.* **1958**, *91*, 380–392.

SCHEME 3. Molecular Machinery on the Mannosyl [c2]Daisy Chains 1a,b and 2a,b Containing, Respectively, Two and Three Molecular Stations for the DB24C8 Derivative

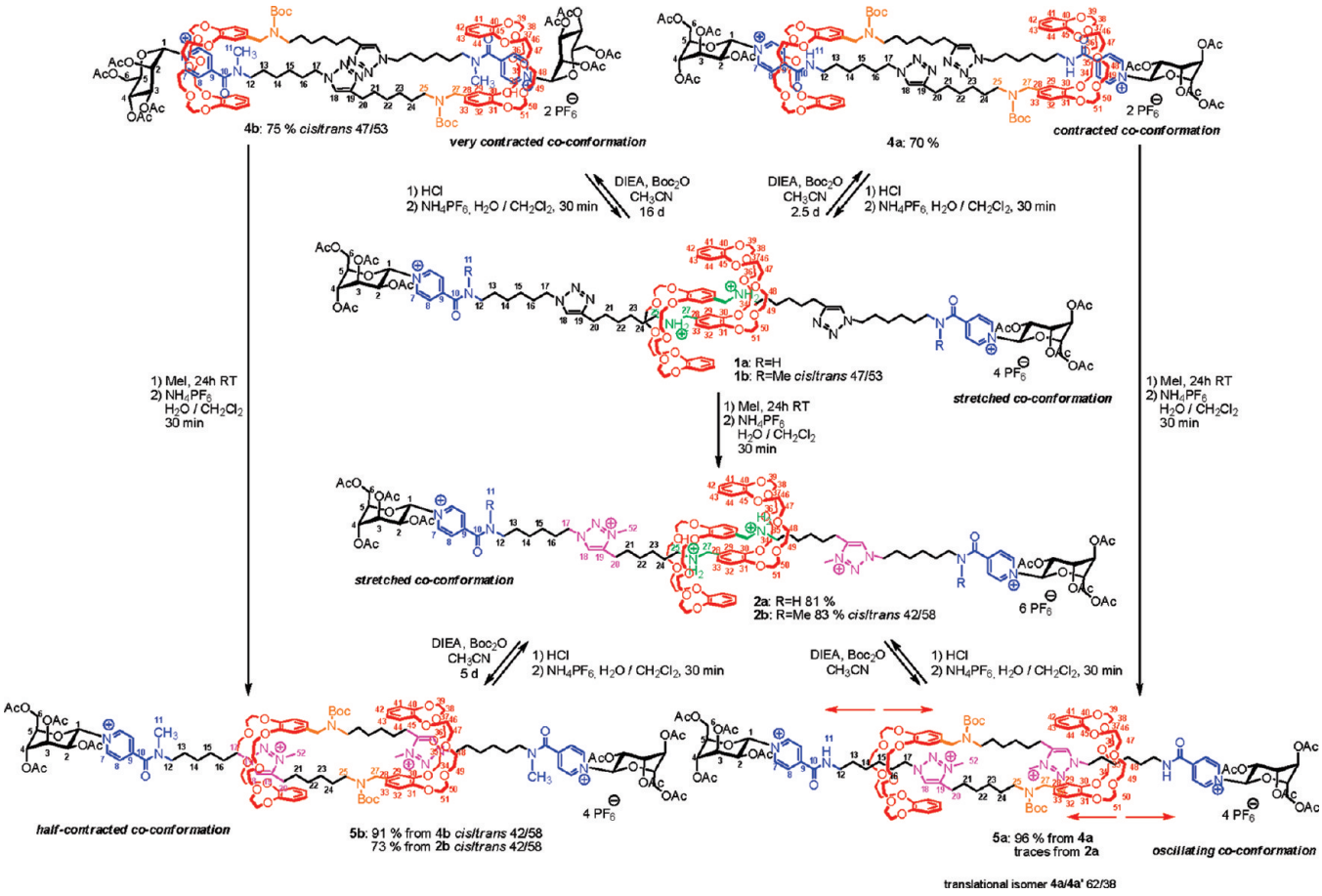

DB24C8. Simultaneously, H_{25} and H_{27} are shifted downfield in the [c2]daisy chain **1a** ($\Delta\delta = +0.44$ and $+0.42$ ppm, respectively), whereas no other significant variations of chemical shifts are observed for the other hydrogens of the axles and more especially for H_{7-8} belonging to the pyridinium amide station, thus indicating the unique localization of the DB24C8 parts around the best ammonium station, and demonstrating a stretched *co*-conformation of **1a**.

After deprotonation−carbamoylation, the two macrocycles glide along the thread until the monosubstituted pyridinium amide station, where they exclusively reside (Scheme 3, Figure 2b,c). This is confirmed by the upfield shift of H_{25} and H_{27} ($\Delta\delta = -0.31$ and -0.19 ppm, respectively), due to the deprotonation−carbamoylation of the ammonium moiety and the shuttling of the DB24C8 ring, and more interestingly by the dramatic downfield shift of the pyridinium amide hydrogens H_8 ($\Delta\delta = +1.00$ ppm) and to a lesser extent H_{11} ($\Delta\delta = +0.29$ ppm). It is noteworthy that no significant variation of chemical shift is observed for H_7, indicating an accurate localization of the macrocycle parts around the sole H_8 and H_{11} belonging to the monosubstituted pyridinium amide station. Another important observation is the downfield shift of the aromatic hydrogens H_{29}, H_{33}, H_{41-44}, and more specifically H_{32} of the DB24C8 arising from the disappearance of the "sandwich"-like stretched *co*-conformation. Concerning the NMR signals of the methylenic hydrogens H_{36-37} and H_{48-49} belonging to the DB24C8, they are shifted upfield, probably because they experience the shielding effect of the aromatic pyridinium ring. Eventually, hydrogens H_{12-16} are all more or less shifted upfield in **4a** because they are localized in the shielding cavity of the aromatic ring of the DB24C8 parts. The same trend is observed by comparing the ^{1}H NMR spectra of the [c2]daisy chain **4a** and the monomer analogue **4au**, thus corroborating the contracted *co*-conformation of **4a** (Figure 2c,d).

b. Molecular Machinery of the Molecular Muscle Mimic System 1b/4b. In the protonated rotaxane dimer **1b**, and similarly to **1a**, the DB24C8 parts only interact with the ammonium station. It results a stretched *co*-conformation of the interwoven architecture (Scheme 3, Figure 3a,b). Here, it is noteworthy that a mixture of two isomers in the *ratio* 47/53 was observed, resulting from the *cis*/*trans* isomerization of the disubstituted amide bond. Each conformer was unambiguously assigned thanks to a 2D-NOESY ^{1}H NMR experiment.

After deprotonation−carbamoylation, the macrocycles shuttle toward the disubstituted pyridinium amide, where they reside exclusively. This was demonstrated by the direct comparison of ^{1}H NMR spectra of rotaxane dimers **1b** and **4b** (Figure 3b,c). The hydrogens H_{25} and H_{27}, located next to the ammonium moiety, are shifted upfield ($\Delta\delta = -0.30$ and -0.17 ppm, respectively) because of the deprotonation−carbamoylation of the ammonium and the shuttling of the macrocycles. In the meantime, and in contrast with the previous molecular machine system **1a**/**4a**, no variation of

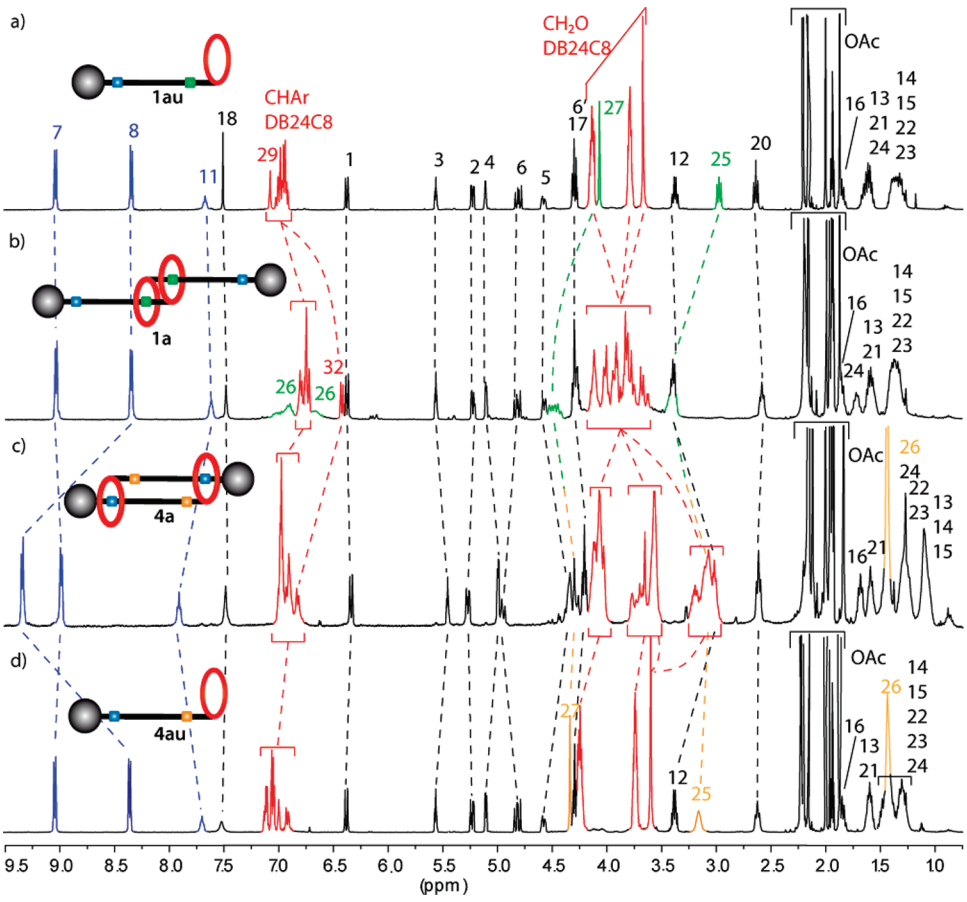

FIGURE 2. ^{1}H NMR spectra (400 MHz, CD_3CN, 298 K) of (a) the uncomplexed monomer **1au**, (b) the protonated mannosyl [c2]daisy chain **1a**, (c) the *N*-Boc mannosyl [c2]daisy chain **4a**, and (d) the uncomplexed *N*-Boc monomer **4au**. The numbering and coloring correspond to the hydrogen assignments indicated in Scheme 3.

chemical shift is observed for H_8. Instead, H_7 is dramatically shifted downfield in both the *trans* and the *cis* isomers ($\Delta\delta$ = +0.91 and +0.96 ppm), revealing their strong implication in hydrogen bonding with the DB24C8, and therefore, the new localization of the macrocycle around the pyridinium unit, but closer to the mannose moiety. Concerning the chemical shifts of the hydrogens belonging to the DB24C8 part, they also undergo important changes. First, the aromatic hydrogens H_{29}, H_{33}, H_{41-44}, and more specifically H_{32} of the DB24C8 are deshielded in **4b** because of the disappearance of the "sandwich"-like stretched *co*-conformation. Second, the ^{1}H NMR signals of the methylenic hydrogens H_{36-37} and H_{48-49} are shifted upfield, probably because they experience the shielding effect of the aromatic pyridinium ring.

Very interestingly, the shuttling of the macrocycles from the ammonium station to the pyridinium station brought about an impressive and tremendous variation of the chair-like conformation of the mannopyranosyl extremities. This was evidenced by the important variations of both the chemical shifts and the coupling constants of the mannopyranosyl skeleton hydrogens H_1-H_6 (Figure 4).

Although no significant variation of chemical shift is observed for H_1, the hydrogens H_3, H_5, and H_6 are all shifted upfield, whereas H_2 and to a lesser extent H_4 are shifted downfield. More significantly, the measured vicinal coupling constant between H_1 and H_2 (9.0 Hz) in the [c2]daisy chain **1b**, dramatically falls to 0 Hz (broad singlet due to the overlapping of the signals of H_1 for the two *cis*/*trans* amide bond containing-isomers) in the carbamoylated [c2]daisy chain **4b**. At the same time, the initial vicinal coupling constants between, respectively, H_3 and H_4 (3.5 Hz) and H_4 and H_5 (1.6 Hz) importantly rise to 8.0 Hz.

In the cyclohexane ring, the theoretical values for vicinal coupling constants of hydrogens located both in axial positions are generally 8−10 Hz and usually become 2−4 Hz if at least one of the two vicinal hydrogens is in an equatorial position.[14] This variation of coupling constants observed between **1b** and **4b** unambiguously indicates the conformational change of the mannopyranose from the $^1C_4$ to the $^4C_1$ conformation. The $^1C_4$ chair conformation observed for the mannopyranose rings in the [c2]daisy chain **1b**[15] was already reported in the literature with simpler mannosylpyridinium. It is actually known that glycosyl pyridinium compounds undergo the controversial reverse anomeric effect (RAE) because a cationic charge, located at the anomeric position of a glucide, forces the aglycon chain to sit in the energetically preferred equatorial position, even though more protected hydroxyl groups are in axial orientations on the pyranose.[16]

(14) Silverstein, R. M.; Webster, F. X.; Kiemle, D. J. *Spectrophotometric Identification of Organic Compounds*, 7th ed.; Wiley: New York, 2005; p 172.
(15) The $^1C_4$ conformation of the chairlike mannopyranose was equally observed in compounds **6a**,**b**, **1a**,**b**, **2a**,**b**, **4a**, and **5a**,**b**.
(16) (a) Perrin, C. L. *Tetrahedron* **1995**, *51*, 11901–11935. (b) Lemieux, R. U.; Morgan, A. R. *Can. J. Chem.* **1965**, *43*, 2205–2213. (c) Lemieux, R. U. *Pure Appl. Chem.* **1971**, *43*, 527–547.

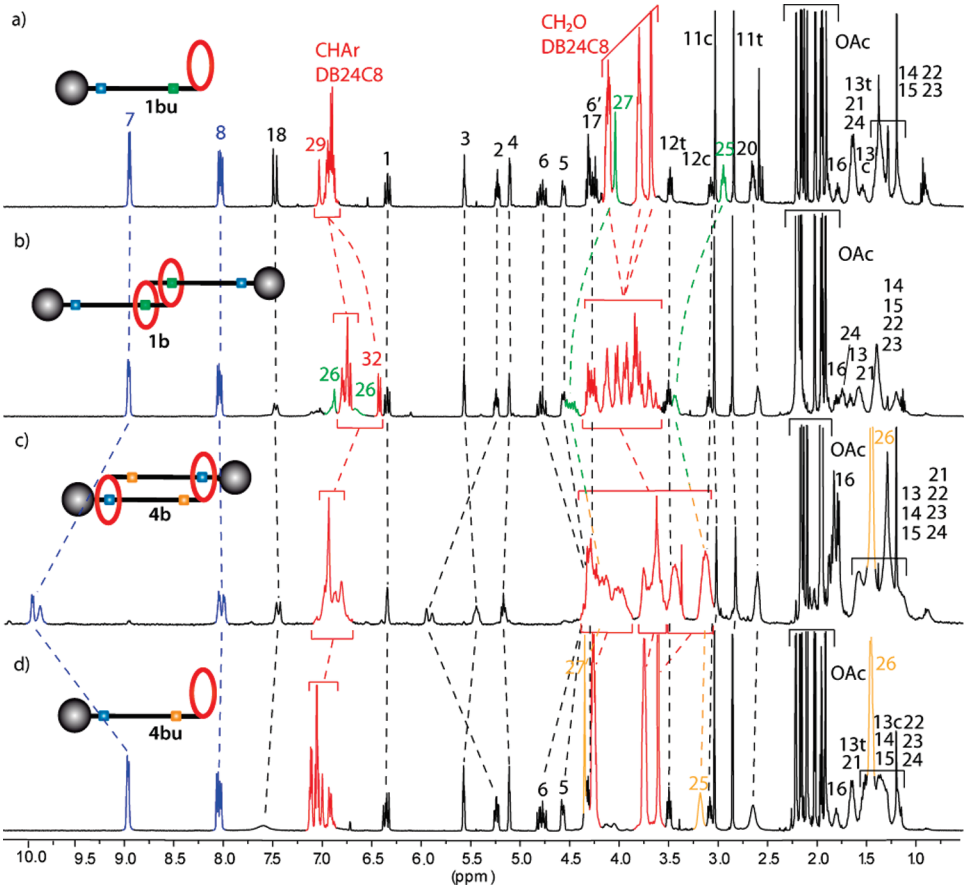

FIGURE 3. ^{1}H NMR spectra (400 MHz, CD_3CN, 298 K) of (a) the uncomplexed monomer **1bu**, (b) the protonated mannosyl [c2]daisy chain **1b**, (c) the *N*-Boc mannosyl [c2]daisy chain **4b**, and (d) the uncomplexed *N*-Boc monomer **4bu**. The numbering and coloring correspond to the hydrogen assignments indicated in Scheme 3.

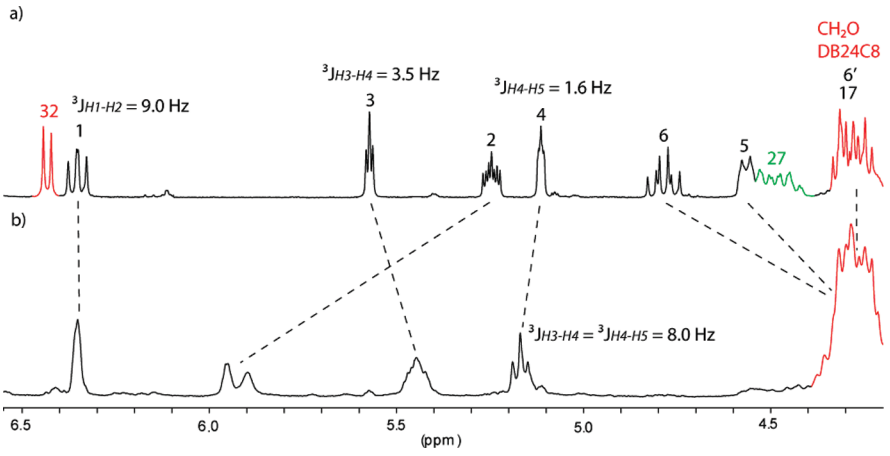

FIGURE 4. ^{1}H NMR partial expanded spectra (400 MHz, CD_3CN, 298 K) of (a) the protonated mannosyl [c2]daisy chain **1b** and (b) the *N*-Boc mannosyl [c2]daisy chain **4b**. The numbering and coloring correspond to the hydrogen assignments indicated in Scheme 3.

In our case, one can assume that the reverse anomeric effect observed in **1b** is switched off in **4b** due to the masking of the cationic charge of the pyridinium and the implication of H_7 in hydrogen bonding with the DB24C8. Eventually, the direct comparison between ^{1}H NMR spectra of [c2]daisy chain **4b** and monomer **4bu** confirmed, on one hand, the localization of the DB24C8 rings around the hydrogens H_7 belonging to the pyridinium station and, on the other hand, the flipping of the mannopyranose chairlike conformation to the $^{4}C_1$ conformation in **4b** (Figure 3c,d).

To summary, the molecular [c2]daisy chain shuttling system **1b**/**4b** exist in either the stretched and the very contracted *co*-conformations. A *domino* effect from one extremity to the other was also observed. Indeed, the deprotonation−carbamoylation sequence applied to the ammonium station at one extremity of the molecule imposes the

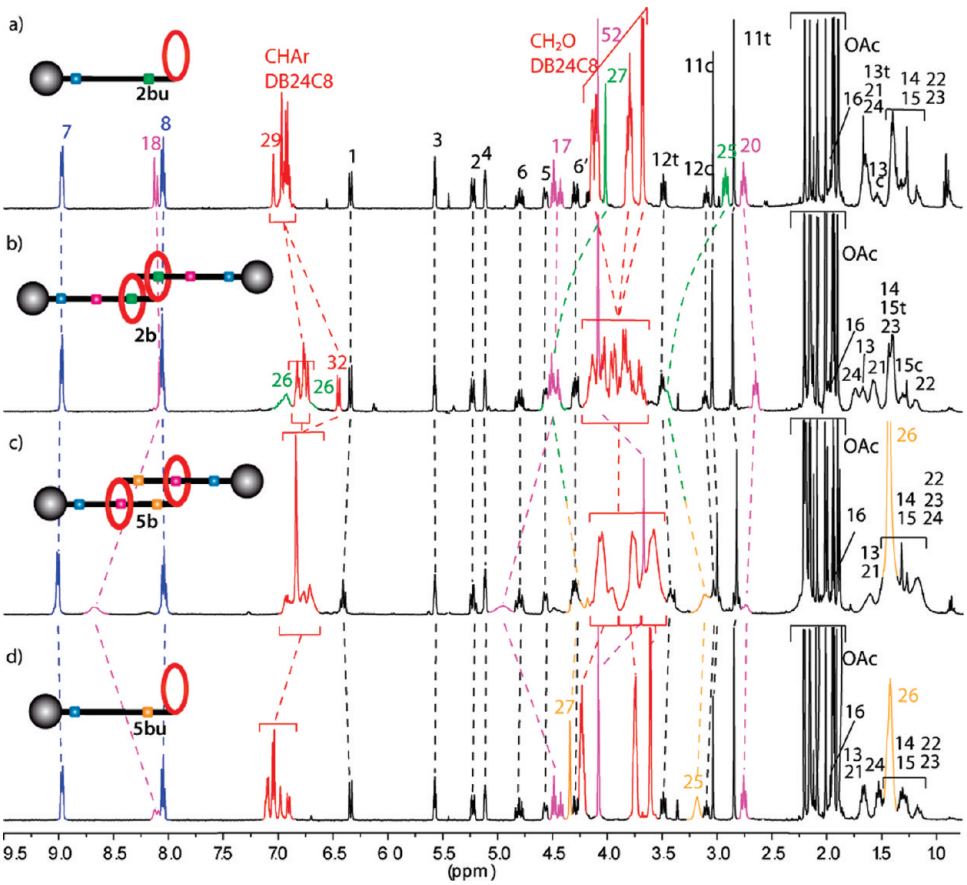

FIGURE 5. ^{1}H NMR spectra (400 MHz, CD_3CN, 298 K) of (a) the uncomplexed monomer **2bu**, (b) the protonated mannosyl [c2]daisy chain **2b**, (c) the *N*-Boc mannosyl [c2]daisy chain **5b**, and (d) the uncomplexed *N*-Boc monomer **5bu**. The numbering and coloring correspond to the hydrogen assignments indicated in Scheme 3.

impressive conformational change of the mannopyranosyl at the other extremity, thanks to the shuttling of the macrocycles.

c. Molecular Machinery of the Molecular Muscle Mimic System 2b/5b. In the three stations—including [c2]daisy chains **2b**/**5b**, the DB24C8 parts are initially localized around the best ammonium stations and force the molecule to adopt a stretched *co*-conformation (Scheme 3). However, upon deprotonation−carbamoylation, the movement of the DB24C8 along the thread appears to be quite different compared to the large amplitude two stations [c2]daisy chain molecular machines **1**/**4**, and the shuttling of the macrocycle directly depends here on the relative affinity of the DB24C8 for the disubstituted pyridinium amide and the triazolium stations. When the [c2]daisy chain **2b** was deprotonated and carbamoylated to give **5b**, the DB24C8 shuttled from the ammonium to the triazolium interaction site, as a result of the better affinity of the DB24C8 for this molecular station than for the disubstituted pyridinium amide. It implicated a half-contracted *co*-conformation of the rotaxane dimer **5b**. This observation was evidenced by the comparison of the ^{1}H NMR spectra of the uncomplexed monomer **2bu**, the protonated rotaxane dimer **2b**, the carbamoylated rotaxane dimer **5b**, and the carbamoylated monomer **5bu** (Figure 5).

By comparing the ^{1}H NMR spectra of **2bu** and **2b**, it is possible to accurately localize the DB24C8 parts around the best ammonium station. Indeed, apart from the hydrogens H_{25} and H_{27}, which are shifted downfield in **2b** ($\Delta\delta = +0.54$ and +0.48 ppm, respectively), due to their hydrogen-bonding interaction with the oxygens of the DB24C8, no other variations of chemical shift are observed for the hydrogens belonging to the two other molecular stations. Concerning the hydrogens of the DB24C8 parts in the [c2]daisy chain **2b**, the same trend of variations is observed than in **1a** and **1b**: the aromatic hydrogens of the DB24C8 are shielded because of a "sandwich"-like assembling structure, and the methylenic hydrogens of the crown ether are split due to the interlocked structure. After deprotonation−carbamoylation, and similarly to the already described molecular machines, H_{25} and H_{27}, which are located next to the ammonium station, are shifted upfield ($\Delta\delta = -0.36$ and −0.29 ppm, respectively), due to the deprotonation of the ammonium group and the shuttling of the DB24C8 parts (Figure 5b,c). Interestingly, and contrary to the previously studied [c2]daisy chain molecular machines **1a**/**4a** and **1b**/**4b**, no variations of chemical shifts for hydrogens H_7 and H_8 belonging to the pyridinium amide unit are observed in **5b**, whereas the hydrogens H_{17}, H_{18} of the triazolium unit are shifted downfield ($\Delta\delta = +0.47$ and +0.61 ppm, respectively) as a result of their hydrogen-bonding implication with the oxygens of the crown ether. At the same time, the methylic triazolium hydrogens H_{52} are dramatically shifted upfield in **5b** ($\Delta\delta = -0.41$ ppm) because of their localization in the shielding cavity of the aromatic ring of the crown ether parts. Concerning the aromatic

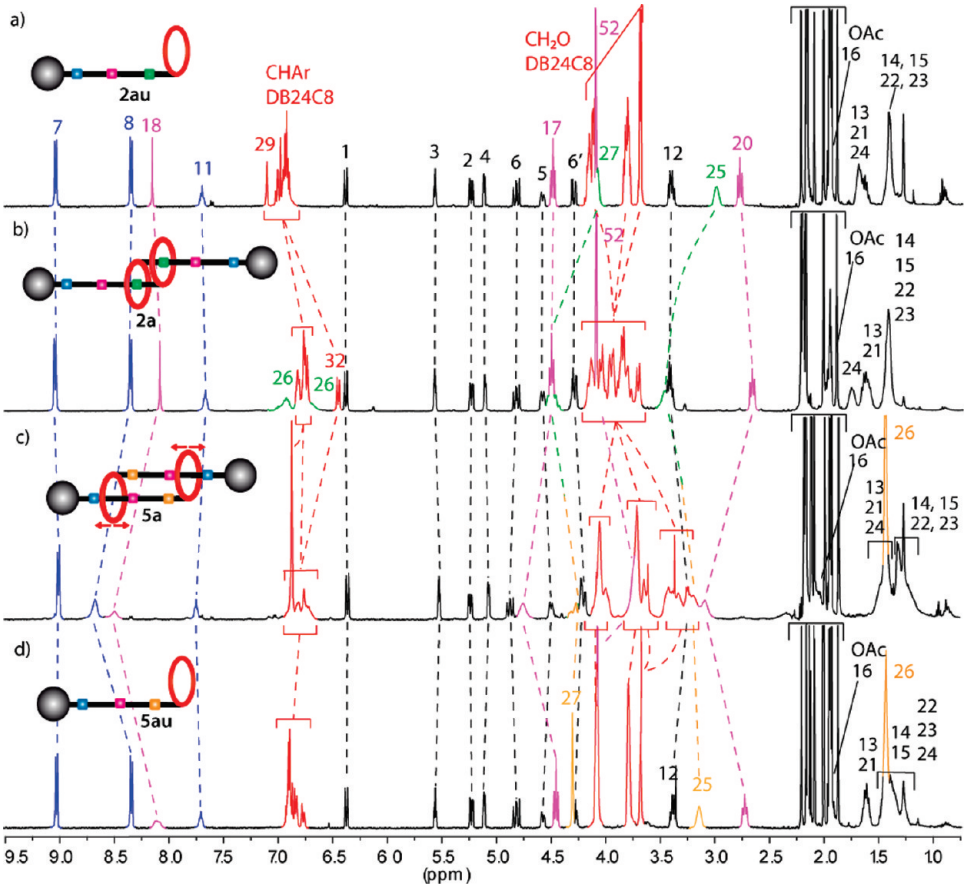

FIGURE 6. ^{1}H NMR spectra (400 MHz, CD_3CN, 298 K) of (a) the uncomplexed monomer **2au**, (b) the protonated mannosyl [c2]daisy chain **2a**, (c) the *N*-Boc mannosyl [c2]daisy chain **5a**, and (d) the uncomplexed *N*-Boc monomer **5au**. The numbering and coloring correspond to the hydrogen assignments indicated in Scheme 3.

hydrogens of the DB24C8, they are again deshielded in **5b** as a result of the disappearance of the "sandwich"-like *co*-conformation. However, it is important to notice that the signals of the methylenic hydrogens belonging to the DB24C8 parts are less shielded in **5b** than in the previously discussed [c2]daisy chain **4a** and **4b** because they are obviously not experiencing the shielding effect of the pyridinium aromatic ring. The direct comparison of the ^{1}H NMR spectra of **5b** and **5bu** corroborates the interaction sites implicating the triazoliums and the macrocycles (Figure 5c, d). In summary, all these NMR observations unambiguously demonstrate that **5b** adopts an half-contracted [c2]daisy chain *co*-conformation, where the DB24C8 macrocycle parts exclusively interact with the triazolium molecular station: they highlight as well the higher affinity of the DB24C8 for the triazolium molecular station than for the disubstituted pyridinium amide one.

d. Molecular Machinery of the Molecular Muscle Mimic System 2a/5a Using Chemical *Stimulus* at Room Temperature and Influence of either Solvent or Temperature *Stimuli* on 5a. In the monosubstituted pyridinium amide series, the molecular machine behaves very differently. Indeed, the already discussed stretched *co*-conformation observed in **2a** changed, after deprotonation−carbamoylation, to a continuous oscillating molecular muscle **5a** adopting at room temperature an alterning *co*-conformation between a half-contracted to a contracted *co*-conformation, where the DB24C8 interact both with the triazolium and the monosubstituted pyridinium amide stations as a result of a similar affinity of the DB24C8 for the two stations. This was demonstrated by the comparison of the ^{1}H NMR spectra of the uncomplexed monomer **2au**, the protonated rotaxane dimer **2a**, the deprotonated−carbamoylated rotaxane dimer **5a**, and the deprotonated−carbamoylated monomer **5au** (Figure 6). In the protonated ammonium state **2a**, and as observed for the [c2]daisy chain **2b**, the rotaxane dimer adopts a stretched "sandwich"-like *co*-conformation, resulting from the higher affinity of the DB24C8 parts for the ammonium station than for the triazolium and the monopyridinium amide stations. Indeed, in comparison with the monomer **2au**, the hydrogens H_{25} and H_{27} of **2a** are deshielded ($\Delta\delta$ = +0.47 and +0.45 ppm, respectively) because of their implication in hydrogen bonds and the aromatic hydrogens of the DB24C8 are shielded due to their localization in the shielding cavity of the aromatic ring of the DB24C8 (Figure 6a,b, Scheme 3).

After deprotonation−carbamoylation of the ammonium station, the new localization of the DB24C8 around both the triazolium and the monosubstituted pyridinium amide stations can be deduced from the comparison between the ^{1}H NMR spectra of rotaxane dimers **5a** and **2a** (Figure 6b,c). In the rotaxane dimer **5a**, the disappearance of the ammonium hydrogens and the appearance of the hydrogen signal of the carbamoylated group H_{26} are accompanied by the usual upfield shift of the hydrogens H_{25} and H_{27} which are initially

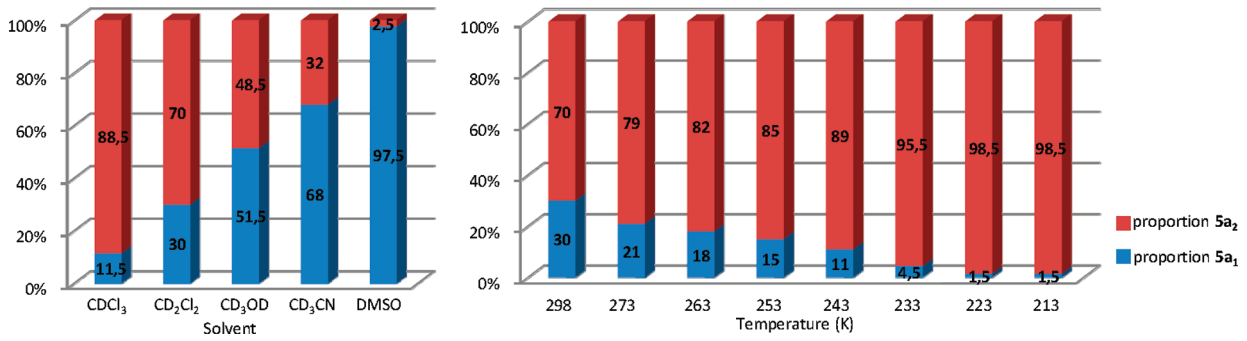

FIGURE 7. Effect of the solvent polarity (at 298 K) and the temperature (in CD_2Cl_2) on the proportions of the translational isomers $\mathbf{5a_1}$ and $\mathbf{5a_2}$.

SCHEME 4. Translational Isomers $\mathbf{5a_1}$/$\mathbf{5a_2}$ Which Are in Fast Exchange at Room Temperature and Comparison with a Simpler [2]Rotaxane A

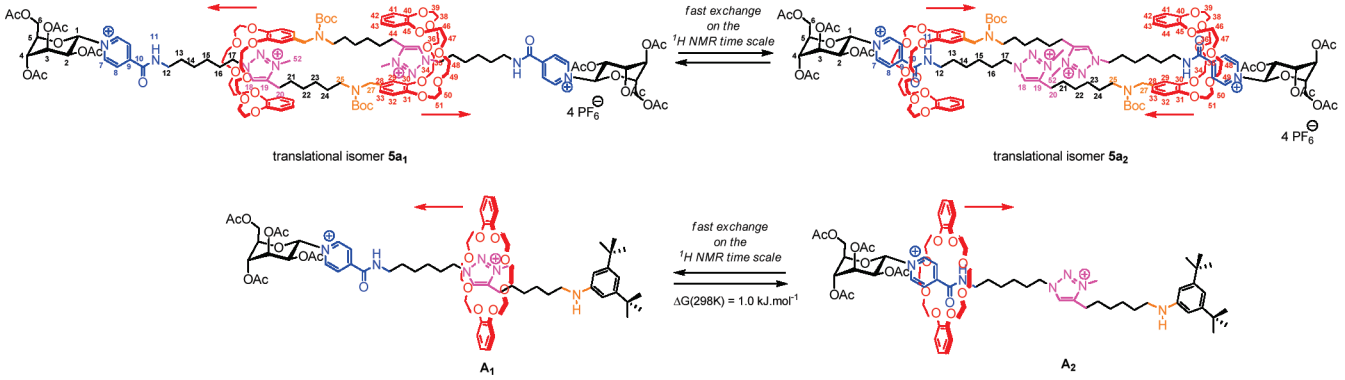

located next to the ammonium moiety. In **5a**, the same downfield shift of H_{32} is observed than the one noticed in all the previously described carbamoylated [c2]daisy chain **4a**, **4b**, and **5b**, whereas the DB24C8 methylenic hydrogens H_{36-37} and H_{48-49} are shielded (more than in **5b**, but a little less than in **4a** and **4b**) since they partially experience the shielding effect of the aromatic pyridinium moiety. Even more interestingly, all of the hydrogens belonging to the two triazolium and monopyridinium amide molecular stations H_{17}, H_{18}, H_{20}, H_8, and H_{11} are shifted downfield in **5a** ($\Delta\delta$ = +0.26, +0.41, +0.44, +0.32, and +0.09 ppm, respectively), indicating their hydrogen-bonding interactions with the oxygens of the DB24C8. It is noteworthy that even though the DB24C8 parts interact with the two molecular stations, only one set of ^{1}H NMR signals is present on the NMR time scale for **5a**. Moreover, the hydrogens, which are implicated in hydrogen-bonding interactions with the DB24C8, are all broadened in **5a**, assuming a continuous fast oscillation of the macrocycles on the NMR time scale at room temperature between the triazolium and the monosubstituted pyridinium amide stations, resulting in a molecular muscle continuously changing its *co*-conformation from a half-contracted to a contracted one. This result is confirmed by the direct comparison between the ^{1}H NMR spectra of **5a** and the monomer **5au** (Figure 6c,d).

The proportion at room temperature of the two translational isomers $\mathbf{5a_1}$/$\mathbf{5a_2}$ of the carbamoylated molecular muscle **5a**, which are in fast exchange on the NMR time scale, was evaluated thanks to the known chemical shift of hydrogens H_8 and H_{18} (which are directly relevant to the two translational isomers $\mathbf{5a_1}$ and $\mathbf{5a_2}$) when they are not engaged in any hydrogen bonding interactions (i.e., in monomers **2au** and **5au**) and when they are totally engaged in hydrogen bonding with the DB24C8 (i.e., in rotaxane dimer **4a** for H_8 and rotaxane dimer **5b** for H_{18}) (Scheme 4, Figure 7).

Surprisingly, an average *ratio* of 68:32 in favor of the half contracted *co*-conformation $\mathbf{5a_1}$ was determined at room temperature in CD_3CN, although it was found in parallel in a recent study with a simpler [2]rotaxane analogue **A** that the pyridinium amide was a slightly better station for the DB24C8 than the triazolium one at room temperature.[17] One could have thus assumed similar affinities of the two stations for the DB24C8 parts in our rotaxane dimers **5a** than in our [2]rotaxane monomer analogue **A**. Nevertheless, the possible repulsion between the two triazolium cationic charges in the contracted molecular muscle $\mathbf{5a_2}$, which directly results from the nature of the constrained interwoven dimer structure, should not be energetically favorable and should therefore increase the population of the half-contracted molecular muscle translational isomer $\mathbf{5a_1}$. The population of each translational isomer $\mathbf{5a_1}$ and $\mathbf{5a_2}$ in the oscillating state was further studied in different more or less dissociating solvents and at different temperature: the shuttle oscillation of the DB24C8 around the two molecular stations was found to be solvent[18] and temperature dependent (Figure 7).

Solvent Effect at Room Temperature on Molecular Muscle 5a. Unsurprisingly, with the exception of the DMSO, the

(17) In CD_3CN, a ratio $\mathbf{A_1}$:$\mathbf{A_2}$ of 38:62 in favor of the isomer containing the DB24C8 around the monosubstituted pyridinium amide station was found in a [2]rotaxane containing the two same stations. Busseron, E.; Romuald, C.; Coutrot, F. *Chem.—Eur. J.* **2010**, *16*, 10062–10073.

variation of the polarity of the solvent (from $CDCl_3$ to CD_3CN via CD_2Cl_2 and MeOD) caused negligible variations of chemical shifts for the hydrogens H_8 ($\Delta\delta$ less than 0.07 ppm) in the contracted [c2]daisy chain **4a** and for H_{18} ($\Delta\delta$ less than 0.07 ppm) in the half-contracted [c2]daisy chain **5b**, corroborating that they are strongly interacting by hydrogen bonding with the DB24C8 macrocycle. On the contrary, the chemical shifts of H_8 in the monomer **5au** and H_{18} in the monomer **2au** (up to $\Delta\delta = 0.17$ and 0.30 ppm, respectively) and in the oscillating molecular muscle **5a** (respectively up to $\Delta\delta = 0.43$ and 0.27 ppm) obviously proved to be more sensitive to the nature of the solvent. This is consistent with the better accessibility of the solvent due to the absence of any intramolecular strong hydrogen-bonding interaction in **2au** and **5au** and to the oscillation of the macrocycle in the molecular muscle **5a**. Much more interestingly, contrary to the translational isomeric [2]rotaxanes $\mathbf{A_1}$ and $\mathbf{A_2}$ which are not sensitive at all to the solvent polarity, an unexpected and impressive inversion of the *ratio* $\mathbf{5a_1}$:$\mathbf{5a_2}$ was observed by changing the solvent from the less dissociating $CDCl_3$ to the more dissociating DMSO via the intermediate CD_2Cl_2, MeOD, and CD_3CN (Figure 7). At room temperature in DMSO and CD_3CN, a molecular muscles *ratio* $\mathbf{5a_1}$:$\mathbf{5a_2}$ of, respectively, 97.5:02.5 and 68:32, in favor of the half-contracted *co*-conformation, was evaluated. However, in $CDCl_3$, an inverted molecular muscle's average *ratio* $\mathbf{5a_1}$:$\mathbf{5a_2}$ of 11.5:88.5 in favor of the contracted molecular muscle *co*-conformation was evaluated, suggesting that the energetically unfavorable repulsion of the two triazolium units in the contracted state is a dominant factor in dissociating solvents like DMSO and to a lesser extent CD_3CN, whereas in less dissociating solvent like CD_2Cl_2 and $CDCl_3$, the repulsion between the more diluted positively charged triazolium units constitutes a weaker factor and the higher affinity of the pyridinium amide station for the DB24C8 imposes the localization of the macrocycle derivatives. In the intermediary CD_3OD solvent, a quasi-equimolar *ratio* for $\mathbf{5a_1}$:$\mathbf{5a_2}$ of 51.5:48.5 was detected.

Temperature Effect on Molecular Muscle 5a and Extracted Thermodynamic Parameters. A low variable-temperature ^1H NMR experimental study was conducted both in a dissociating solvent like CD_3CN and in a less dissociating solvent like CD_2Cl_2 with the aim of freezing the system (Scheme 4, Figure 7). Upon decreasing the temperature, the fast-exchange equilibrium between $\mathbf{5a_1}$ and $\mathbf{5a_2}$ clearly shifts toward $\mathbf{5a_2}$. In CD_2Cl_2, decreasing the temperature results in the progressive increase of the population of the translational isomer $\mathbf{5a_2}$ until the macrocycle froze exclusively around the pyridinium amide station (Figure 8). This was demonstrated by the progressive downfield shift of the ^1H NMR signal observed for H_8, until it reached the ^1H NMR chemical shift of H_8 belonging to the contracted *N*-Boc mannosyl [c2]daisy chain **4a** at the same temperature (Figure 8a,b). Parallel to this observation, the ^1H NMR signal for H_{18} is shifted upfield at lower temperature until it reaches the chemical shift value of H_{18} in the uncomplexed *N*-Boc monomer **2au** (Figure 8a−c). The displacement of the translational isomeric equilibrium occurred in the same way in CD_3CN, however, in a lesser extent, probably because upon decreasing the temperature, the energetic gain, resulting from the translation of the DB24C8 around the monosubstituted pyridinium amide station, is compensated by an energetic unfavorable repulsion of the triazolium stations.

Thermodynamic parameters corresponding to the fast exchange on the NMR time scale between $\mathbf{5a_1}$ and $\mathbf{5a_2}$ were extracted from a Van't Hoff plot[19] (Figure 9) thanks to the thermodynamic constants K[20] determined at different temperatures. The plot appeared linear over the examined range of temperature (with a linear regression coefficient $R_2 = 0.999$) and provided the translational isomeric exchange enthalpy from $\mathbf{5a_2}$ to $\mathbf{5a_1}$ $\Delta H = 12.4\ kJ \cdot mol^{-1}$ and entropy $\Delta S = 34.4\ J \cdot K^{-1} \cdot mol^{-1}$. A free Gibbs energy ΔG (298K) of $2.1\ kJ \cdot mol^{-1}$ was calculated, indicating the more energetically favorable translational isomer $\mathbf{5a_2}$ due to the slightly better affinity of the DB24C8 for the monosubstituted pyridinium amide unit. It is interesting to note that this energy is twice the value found for the exchange between translational isomers of the simpler monomeric [2]rotaxane analogues **A**.

DB24C8 Macrocycle as a Molecular Brake for the Rotation of the C_9-C_{10} Bond. Eventually, in CD_2Cl_2, hydrogens H_8 belonging to the oscillating rotaxane **5a** appear as single NMR frequency above 213 K, whereas they coalesce at a temperature of 213 K and are split at lower temperature (Figure 8). This is attributed to the decrease of the rotation rate of the bond C_9-C_{10} between the pyridinium and the amide carbonyl when lowering temperature, due to the anchoring of the macrocycles at the two H-bonding sites surrounding the C_9-C_{10} linkage. Above 213 K, the rotation of the link C_9-C_{10} is fast on the NMR time scale, whereas it becomes slow below 213 K. Remarkably, no coalescence of H_8 is observed either for the monomeric noninterlocked analogues **2au** and **5au** and the half-contracted [c2]daisy chain **5b**, where the DB24C8 moieties sit around the triazolium stations, highlighting the role of molecular brake of the DB24C8 in the rotation of the covalent bond C_9-C_{10} when the macrocycles are located around both the pyridinium and the monosubstituted amide hydrogens. At 213 K, a rate constant for the rotational isomeric exchange of $290\ s^{-1}$ was provided by the equation $k_{rot} = \pi\delta\nu/\sqrt{2}$,[21] where $\delta\nu$ (130.6 Hz) corresponds to the line width at half-height of the coalesced NMR signal for H_8. This kinetic rate gave access to the free energy of activation between the rotamers $\Delta G_{rot}^{\ddagger}{}_{213} = 41.5\ kJ \cdot mol^{-1}$.[22]

Conclusions

Four new [c2]daisy chain molecular machines based on a DB24C8 macrocycle and containing two or three stations,

(18) For other solvent-dependent molecular switches, see: (a) Lane, S. A.; Leigh, D. A.; Murphy, A. J. *J. Am. Chem. Soc.* **1997**, *119*, 11092–11093. (b) Tzu-Chiun, L.; Chien-Chen, L.; Sheng-Hsien, C. *Org. Lett.* **2009**, *11*, 613–616. (c) Ambrosi, G.; Dapporto, P.; Formica, M.; Fusi, V.; Giorgi, L.; Guerri, A.; Micheloni, M.; Paoli, P.; Pontellini, R.; Rossi, P. *Chem.—Eur. J.* **2003**, *9*, 800–810. (d) Chiang, P.-T.; Cheng, P.-N.; Lin, C.-F.; Liu, Y.-H.; Lai, C.-C.; Peng, S.-M.; Chiu, S.-H. *Chem.—Eur. J.* **2006**, *12*, 865–876. (e) Hannam, J. S.; Kidd, T. J.; Leigh, D. A.; Wilson, A. J. *Org. Lett.* **2003**, *5*, 1907–1910.

(19) Pastor, A.; Martinez-Viviente, E. *Coord. Chem. Rev.* **2008**, *252*, 2314–2345.

(20) Thermodynamic constants K were calculated from the mean proportions of $\mathbf{5a_1}/\mathbf{5a_2}$ which were determined from both ^1H NMR signals H_8 and H_{18}.

(21) *Dynamic NMR Spectroscopy*; Sandstrom, J., Ed.; Academic Press: New York, 1982.

(22) The free enthalpy of activation was calculated using the Eyring equation: $\Delta G^{\ddagger}_{T} = -RT\ln(kh/k_bT)$.

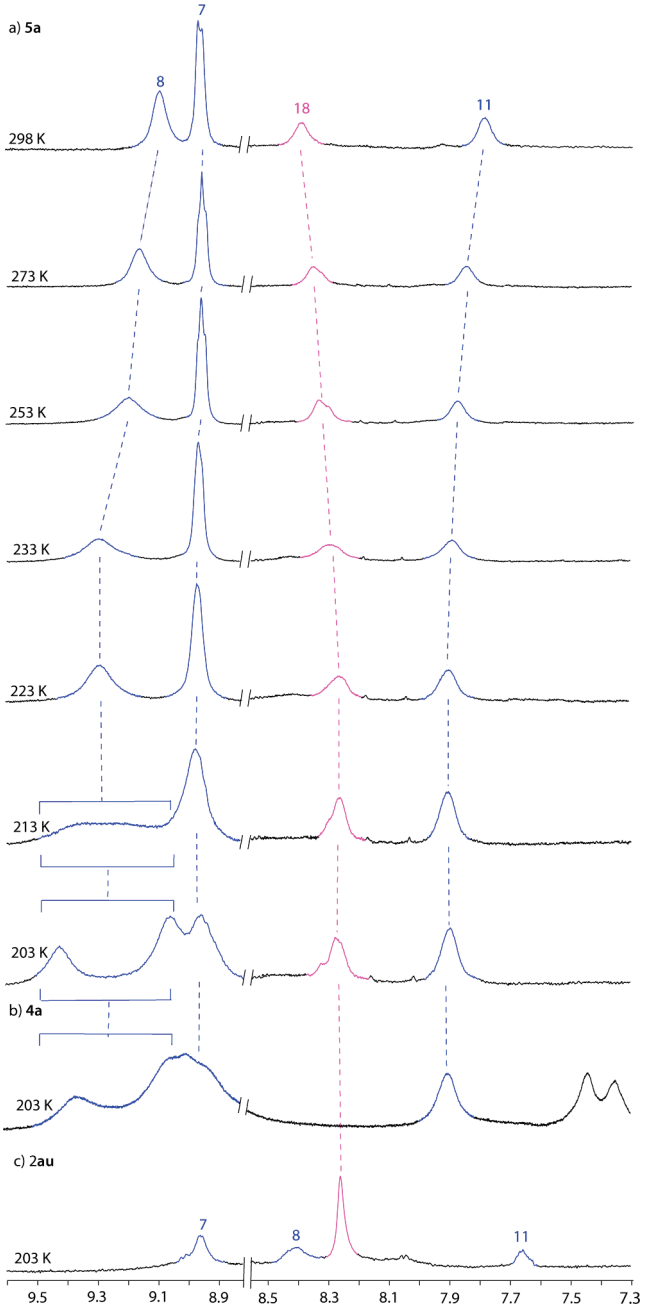

FIGURE 8. Partial ^{1}H NMR spectra (400 MHz, CD_2Cl_2) of (a) the oscillating *N*-Boc mannosyl [c2]daisy chain **5a** at different temperatures; (b) the contracted *N*-Boc mannosyl [c2]daisy chain **4a** at 203 K; and (c) the uncomplexed monomer **2au** at 203 K. The numbering and coloring correspond to the hydrogen assignments indicated in Scheme 3.

among an ammonium, a triazolium, and a mono- or a disubstituted pyridinium amide stations, have been prepared and studied. They gave rise to molecular machines which are triggered by deprotonation−carbamoylation, solvent polarity, and temperature. Two large-amplitude molecular muscles, from stretched to contracted or very contracted *co*-conformations, could be obtained using two molecular stations for the DB24C8. They both behave differently depending on the substitution of the pyridinium amide. In the presence of the monosubstituted pyridinium amide station, a contracted state

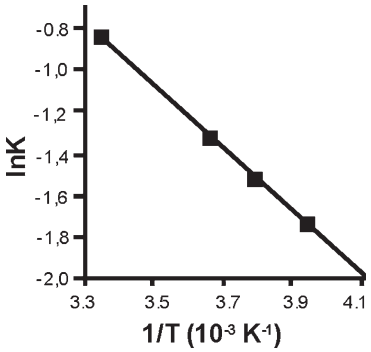

FIGURE 9. Thermodynamic Van't Hoff plot for the translational isomeric exchange between $\mathbf{5a_1}$ and $\mathbf{5a_2}$ in CD_2Cl_2 (253−298 K).

was reached. However, in the presence of the disubstituted pyridinium amide station, the macrocycles shuttled toward a slightly different very contracted state and triggered an impressive flipping of the chairlike mannopyranose extremity by turning off the reverse anomeric effect. Incorporation of a third station (i.e., triazolium) allowed us to reach two new molecular machines. A half-contracted *co*-conformation was possible with the disubstituted pyridinium amide station, whereas in the monosubstituted pyridinium amide station series, an interesting oscillating molecular muscle occurred. The continuous oscillation of the DB24C8 between the triazolium and the monosubstituted pyridinium amide stations could be highly controlled by the variation of the solvent polarity or by the temperature. In a dissociating solvent like DMSO, the higher repulsion between triazolium moieties favors the half-contracted translational isomer, even though the pyridinium amide station has a slightly better affinity for the DB24C8 than the triazolium. On the contrary, the nondissociating solvents like $CDCl_3$ favor the contracted translational isomer because the stabilization by hydrogen bonding between the DB24C8 and the best pyridinium amide station is not compensated by the repulsion of the triazolium, which is actually much lower due to a more diluted cationic charge. In CD_2Cl_2, when no such triazolium repulsion occurred, the decrease of the temperature highly displaced the translational exchange equilibrium from the half-contracted to the unique energetically favorable contracted state, until no more oscillation persists. Thermodynamic parameters could then be extracted from the variable-temperature NMR study and provided the free Gibbs energy of the translational equilibrium, which exactly matches to twice the free Gibbs energy calculated for a simpler analogous monomeric [2]rotaxane. Finally, it was demonstrated the molecular brake role of the DB24C8 when it is located around the monosubstituted pyridinium amide moiety: it caused a tremendous decrease of the rotation of the surrounded bond C_9-C_{10}. Improving the knowledge of the behaviors of molecular muscles, depending on the nature and the number of stations, may prove useful for the development of new molecular switches.

Experimental Section

All reactions were carried out under an atmosphere of argon unless otherwise indicated. The reagents were used as received without further purification. Dichloromethane was distilled over P_2O_5 and was degassed by bubbling Ar for 20 min. Analytical thin-layer chromatography (TLC) was performed

on silica gel 60 F254 plates. Compounds were visualized by dipping the plates in an ethanolic solution of 10% sulfuric acid, ninhydrin, or an aqueous solution of $KMNO_4$, followed by heating. ^1H NMR and ^{13}C NMR spectra were obtained at 400.13 and 100.62 MHz, respectively. Chemical shifts of ^1H NMR and ^{13}C NMR are given by using $CHCl_3$ CH_2Cl_2, DMSO, MeOH, or CH_3CN as references (7.27, 5.32, 2.50, 3.31, or 1.94 ppm, respectively, for the ^1H spectrum, and 77 and 118.26 ppm, respectively, for the ^{13}C spectrum in $CDCl_3$ and CD_3CN). ^1H assignments were deduced from 2D $^1H-^1H$ NMR COSY experiments. ^{13}C assignments were deduced from 2D $^{13}C-^1H$ NMR HMQC experiments. Coupling constants (J) are reported in hertz (Hz). Standard abbreviations indicating multiplicity were used as follows: s (singlet), br (broad), d (doublet), t (triplet), q (quartet), m (multiplet). Mass spectra (MS) and high-resolution mass spectra (HRMS) were recorded, respectively, on a ZQ Micromass apparatus and a Q-TOF Micro apparatus.

1. Starting Materials and Monomers. The preparations of the precursor compounds **6a**,**b** and **7** are described in detail in the Supporting Information. The syntheses of monomers **1au**, **1bu**, **2au**, **2bu**, **4au**, **4bu**, **5au**, and **5bu** are reported in the Supporting Information.

2. Synthesis of Rotaxane Dimers. 2.1. Rotaxane Dimers 1a and 1b. In a typical procedure, $Cu(CH_3CN)_4PF_6$ (153 mg, 0.410 mmol 1 equiv) and 2,6-lutidine (4.4 μL, 0.041 mmol, 0.1 equiv) were added successively to a solution of the azido compound **6a** (297 mg, 0.410 mmol, 1 equiv) and the alkyne compound **7** (300 mg, 0.410 mmol, 1 equiv) in 3 mL of dry dichloromethane. The mixture was stirred for 24 h at room temperature, after which time the solvent was evaporated in vacuo. The crude was then directly purified by chromatography on a silica gel column (solvent gradient elution CH_2Cl_2/MeOH 98:2 to 85:15) to afford the rotaxane dimer **1a** as a yellow solid.

a. The rotaxane Dimer **1a** (R = H) was obtained in a77% yield. R_f (CH_2Cl_2/MeOH 9:1): 0.26. ^1H NMR (400 MHz, CD_3CN, 298 K): δ (ppm) 9.04 (d, 4H, $^3J_{H7-H8}$ = 6.6 Hz, H_7), 8.35 (d, 4H, $^3J_{H8-H7}$ = 6.6 Hz, H_8), 7.66−7.58 (br t, 2H, H_{11}), 7.48 (s, 2H, H_{18}), 6.99−6.85 and 6.73−6.55 (2 m, 4H, H_{26}), 6.84−6.70 (m, 12H, H_{29} H_{33} H_{41} H_{42} H_{43} H_{44}), 6.42 (d, 2H, $^3J_{H32-H33}$ = 8.3 Hz, H_{32}), 6.38 (d, 2H, $^3J_{H1-H2}$ = 9.0 Hz, H_1), 5.56 (t, 2H, $^3J_{H3-H2}$ = $^3J_{H3-H4}$ = 3.2 Hz, H_3), 5.23 (dd, 2H, $^3J_{H2-H1}$=9.0 Hz, $^3J_{H2-H3}$=3.2 Hz, H_2), 5.11 (dd, 2H, $^3J_{H4-H3}$ = 3.2 Hz, $^3J_{H4-H5}$ = 2.0 Hz, H_4), 4.82 (dd, 2H, $^3J_{H6-H5}$ = 9.2 Hz, $^2J_{H6-H6'}$ = 12.7 Hz, H_6), 4.60−4.55 (m, 2H, H_5), 4.58−4.40 (m, 4H, H_{27}), 4.34−4.22 (m, 6H, $H_{6'}$ H_{17}), 4.17−3.60 (m, 48H, CH_2O), 3.48−3.33 (m, 8H, H_{12} H_{25}), 2.58 (t, 4H, $^3J_{H20-H21}$ = 7.4 Hz, H_{20}), 2.20 and 2.16 and 2.00 and 1.86 (4*s, 24H, CH_3CO), 1.90−1.83 (m, 4H, H_{16}), 1.77−1.66 (m, 4H, H_{24}), 1.66−1.51 (m, 8H, H_{13} H_{21}), 1.46−1.26 (m, 16H, H_{14} H_{15} H_{22} H_{23}). JMOD ^{13}C NMR (100 MHz, CD_3CN, 298 K): δ (ppm) = 171.5, 170.3 and 170.0, 169.9 ($COCH_3$), 162.4 (C_{10}), 153.0 (C_9), 148.6 and 147.0 and 146.9 (C_{19} C_{30} C_{31} C_{40} C_{45}), 144.1 (C_7), 127.2 (C_8), 126.2 (C_{28}), 123.5 and 123.5 and 121.5 and 121.5 and 114.1 and 112.9 and 112.6 and 112.6 (C_{29} C_{32} C_{33} C_{41} C_{42} C_{43} C_{44}), 89.0 (C_1), 78.7 (C_5), 72.9 and 72.9 and 71.4 and 71.3 and 71.2 and 71.0 and 68.4 and 68.4 and 68.1 and 68.0 and 68.0 and 67.8 (CH_2O), 69.6 (C_2), 68.2 (C_4), 67.4 (C_3), 60.9 (C_6) 52.7 (C_{27}), 50.6 (C_{17}), 49.7 (C_{25}), 40.9 (C_{12}), 30.8 (C_{16}), 29.9 and 29.4 and 29.0 and 27.2 and 26.9 and 26.8 and 26.6 (C_{13} C_{14} C_{15} C_{21} C_{22} C_{23} C_{24}), 25.9 (C_{20}), 21.0 and 20.9 and 20.8 and 20.4 (CH_3CO). HRMS (ESI): $[M - 4PF_6]^{4+}$ calcd for $[C_{118}$ $H_{168}N_{12}O_{36}]^{4+}$ 582.2921, found 582.2929.

b. The rotaxane dimer **1b** (R = Me) was obtained in 74% yield. R_f (CH_2Cl_2/MeOH 9:1): 0.53. Ratio of isomers *cis*/*trans* = 47:53. ^1H NMR (400 MHz, CD_3CN, 298 K): cis isomer δ (ppm) = 8.97 (d, 4H, $^3J_{H7-H8}$ = 6.7 Hz, H_7), 8.04 (d, 4H, $^3J_{H8-H7}$ = 6.7 Hz, H_8), 7.47 (s, 2H, H_{18}), 6.97−6.86 and 6.71−6.60 (2 m, 4H, H_{26}), 6.90−6.70 (m, 12H, H_{29} H_{33} H_{41} H_{42} H_{43} H_{44}), 6.43 (d, 2H, $^3J_{H32-H33}$ = 8.4 Hz, H_{32}), 6.37 (d, 2H, $^3J_{H1-H2}$ = 9.0 Hz, H_1), 5.57 (t, 2H, $^3J_{H3-H2}$ = $^3J_{H3-H4}$ = 3.5 Hz, H_3), 5.26 (dd, 2H, $^3J_{H2-H1}$ = 9.0 Hz, $^3J_{H2-H3}$ = 3.5 Hz, H_2), 5.13−5.10 (m, 2H, H_4), 4.80 (dd, 2H, $^3J_{H6-H5}$=9.0 Hz, $^2J_{H6-H6'}$=12.6 Hz, H_6), 4.59−4.54 (m, 2H, H_5), 4.59−4.41 (m, 4H, H_{27}), 4.35−4.19 (m, 6H, $H_{6'}$ H_{17}), 4.35−3.54 (m, 48H, CH_2O), 3.48−3.38 (m, 4H, H_{25}), 3.08 (t, 4H, $^3J_{H12-H13}$ = 7.4 Hz, H_{12}), 3.03 (s, 6H, H_{11}), 2.63−2.55 (m, 4H, H_{20}), 2.20 and 2.14 and 2.01 and 1.90 (4*s, 24H, CH_3CO), 1.92−1.76 (m, 4H, H_{16}), 1.76−1.70 (m, 4H, H_{24}), 1.61−1.50 (m, 8H, H_{13} H_{21}), 1.46−1.14 (m, 16H, H_{14} H_{15} H_{22} H_{23}); trans isomer δ (ppm) = 8.99 (d, 4H, $^3J_{H7-H8}$ = 6.7 Hz, H_7), 8.07 (d, 4H, $^3J_{H8-H7}$ = 6.7 Hz, H_8), 7.50 (s, 2H, H_{18}), 6.97−6.86 and 6.71−6.60 (2 m, 4H, H_{26}), 6.90−6.70 (m, 12H, H_{29} H_{33} H_{41} H_{42} H_{43} H_{44}), 6.43 (d, 2H, $^3J_{H32-H33}$ = 8.4 Hz, H_{32}), 6.34 (d, 2H, $^3J_{H1-H2}$ = 9.0 Hz, H_1), 5.57 (t, 2H, $^3J_{H3-H2}$ = $^3J_{H3-H4}$ = 3.5 Hz, H_3), 5.23 (dd, 2H, $^3J_{H2-H1}$ = 9.0 Hz, $^3J_{H2-H3}$ = 3.5 Hz, H_2), 5.13−5.10 (m, 2H, H_4), 4.77 (dd, 2H, $^3J_{H6-H5}$ = 9.2 Hz, $^2J_{H6-H6'}$ = 12.6 Hz, H_6), 4.59−4.54 (m, 2H, H_5), 4.59−4.41 (m, 4H, H_{27}), 4.35−4.19 (m, 6H, $H_{6'}$ H_{17}), 4.35−3.54 (m, 48H, CH_2O), 3.50 (t, 4H, $^3J_{H12-H13}$ = 7.3 Hz, H_{12}), 3.48−3.38 (m, 4H, H_{25}), 2.85 (s, 6H, H_{11}), 2.63−2.55 (m, 4H, H_{20}), 2.20 and 2.15 and 2.01 and 1.90 (4*s, 24H, CH_3CO), 1.92−1.76 (m, 4H, H_{16}), 1.76−1.70 (m, 4H, H_{24}), 1.68−1.61 (m, 4H, H_{13}), 1.61−1.50 (m, 4H, H_{21}), 1.46−1.14 (m, 16H, H_{14} H_{15} H_{22} H_{23}). JMOD ^{13}C NMR (100 MHz, CD_3CN, 298 K): δ (ppm) = 171.5 and 170.3 and 170.1 and 170.0 ($COCH_3$), 165.8 and 165.6 (C_{10}), 156.8 and 156.6 (C_9), 148.7 and 147.2 and 147.0 (C_{19} C_{30} C_{31} C_{40} C_{45}), 144.1 and 144.1 (C_7), 127.1 and 126.9 (C_8), 126.3 (C_{28}), 122.4 and 122.2 (C_{18}), 123.6 and 121.6 and 114.2 and 113.0 and 112.7 (C_{29} C_{32} C_{33} C_{41} C_{42} C_{43} C_{44}), 89.3 and 89.2 (C_1), 78.5 and 78.4 (C_5), 73.0 and 71.5 and 71.4 and 71.3 and 71.1 and 68.5 and 68.2 and 68.1 and 68.0 (CH_2O), 69.7 and 69.7 (C_2), 68.3 (C_4), 67.6 and 67.6 (C_3), 61.2 and 61.1 (C_6), 52.8 (C_{27}), 51.3 (C_{12cis}), 48.0 ($C_{12trans}$), 50.5 and 50.4 (C_{17}), 49.7 (C_{25}), 37.1 ($C_{12trans}$), 32.7 (C_{11cis}), 30.9 and 30.7 (C_{16}), 30.1 and 30.0 and 29.2 and 29.1 and 28.3 and 27.3 and 27.2 and 27.1 and 27.0 and 27.0 and 26.8 and 26.8 and 26.7 and 26.3 (C_{13} C_{14} C_{15} C_{21} C_{22} C_{23} C_{24}), 26.0 (C_{20}), 21.0 and 20.9 and 20.8 and 20.6 and 20.6 (CH_3CO). HRMS (ESI): $[M - 4PF_6]^{4+}$ calcd for $[C_{120}$ $H_{172}N_{12}O_{36}]^{4+}$ 589.2999, found 589.2994

2.2. Rotaxane Dimers 2a and 2b. In a typical procedure, rotaxane dimer **1a** (150 mg, 0.0515 mmol) was suspended in 3 mL of iodomethane and stirred for 1 day at room temperature. Iodomethane was then evaporated under reduced pressure, and the obtained solid was washed with diethyl ether to give a yellow solid. NH_4PF_6 (34 mg, 0.206 mmol, 4 equiv) and 2 mL of dichloromethane were added to a suspension of the previous product in 2 mL of Milli-Q water. The resulting bilayer solution was vigorously stirred for 30 min. After separation, the aqueous layer was extracted with 5 mL of dichloromethane. The organic layers were combined, dried over $MgSO_4$, and concentrated to obtain the molecular muscle **2a** (135 mg, 81%) as a yellow solid.

a. The rotaxane dimer **2a** (R = H) was obtained in 81% yield. R_f (CH_2Cl_2/MeOH 9:1): 0.59. ^1H NMR (400 MHz, CD_3CN, 298 K): δ (ppm) = 9.05 (d, 4H, $^3J_{H7-H8}$ = 6.9 Hz, H_7), 8.36 (d, 4H, $^3J_{H8-H7}$ = 6.9 Hz, H_8), 8.09 (s, 2H, H_{18}), 7.72−7.63 (br t, 2H, H_{11}), 6.99−6.87 and 6.74−6.64 (2 m, 4H, H_{26}), 6.87−6.71 (m, 12H, H_{29} H_{33} H_{41} H_{42} H_{43} H_{44}), 6.45 (d, 2H, $^3J_{H32-H33}$ = 8.4 Hz, H_{32}), 6.38 (d, 2H, $^3J_{H1-H2}$ = 9.0 Hz, H_1), 5.57 (t, 2H, $^3J_{H3-H2}$=$^3J_{H3-H4}$=3.4 Hz, H_3), 5.23 (dd, 2H, $^3J_{H2-H1}$ = 9.0 Hz, $^3J_{H2-H3}$ = 3.4 Hz, H_2), 5.11 (dd, 2H, $^3J_{H4-H3}$ = 3.4 Hz, $^3J_{H4-H5}$ = 2.1 Hz, H_4), 4.82 (dd, 2H, $^3J_{H6-H5}$ = 9.2 Hz, $^2J_{H6-H6'}$ = 12.7 Hz, H_6), 4.61−4.55 (m, 2H, H_5), 4.50 (t, 4H, $^3J_{H17-H16}$ = 7.1 Hz, H_{17}), 4.61−4.41 (m, 4H, H_{27}), 4.29 (dd, 2H, $^3J_{H6'-H5}$ = 3.7 Hz, $^2J_{H6'-H6}$ = 12.7 Hz, $H_{6'}$), 4.19−3.65 (m, 48H, CH_2O), 4.09 (s, 6H, H_{52}), 3.52−3.36 (m, 8H, H_{12} H_{25}), 2.65 (t, 4H, $^3J_{H20-H21}$ = 7.9 Hz, H_{20}), 2.21 and 2.16 and 2.00 and 1.88 (4*s, 24H, CH_3CO), 1.99−1.92 (m, 4H, H_{16}), 1.80−1.69 (m, 4H, H_{24}), 1.69−1.53 (m, 8H, H_{13} H_{21}), 1.48−1.35 (m, 16H, H_{14} H_{15} H_{22} H_{23}). JMOD ^{13}C NMR (100 MHz, CD_3CN, 298 K) δ (ppm) = 171.6 and 170.3 and 170.0 and 169.9 ($COCH_3$), 162.5 (C_{10}),

153.0 (C_9), 148.7 and 147.1 and 146.9 and 145.5 (C_{19} C_{30} C_{31} C_{40} C_{45}), 144.1 (C_7), 128.4 (C_{18}), 127.2 (C_8), 126.2 (C_{28}), 123.5 and 121.6 and 114.1 and 113.0 and 112.7 (C_{29} C_{32} C_{33} C_{41} C_{42} C_{43} C_{44}), 89.1 (C_1), 78.7 (C_5), 73.0 and 72.9 and 71.5 and 71.3 and 71.2 and 71.0 and 68.4 and 68.2 and 68.0 and 67.9 (*C*H_2O), 69.6 (C_2), 68.3 (C_4), 67.5 (C_3), 60.9 (C_6), 54.4 (C_{17}), 52.8 (C_{27}), 49.6 (C_{25}), 40.9 (C_{12}), 38.1 (C_{52}), 29.7 (C_{16}), 29.3 and 28.9 and 27.4 and 27.2 and 26.9 and 26.1 (C_{13} C_{14} C_{15} C_{21} C_{22} C_{23} C_{24}), 23.5 (C_{20}), 21.0 and 20.9 and 20.8 and 20.4 (*C*H_3CO). HRMS (ESI): $[M - 3PF_6]^{3+}$ calcd for $[C_{120}H_{174}N_{12}O_{36}\ 3PF_6]^{3+}$ 931.3693, found 931.3714

b. The rotaxane dimer **2b** (R = Me) was obtained in 83% yield. R_f (CH_2Cl_2/MeOH 9:1): 0.46. Ratio of isomers *cis*/*trans* 43:57. ^{1}H NMR (400 MHz, CD_3CN, 298 K): cis isomer δ (ppm) = 8.97 (d, 4H, $^3J_{H7-H8}$ = 6.8 Hz, H_7), 8.06 (s, 2H, H_{18}), 8.05 (d, 4H, $^3J_{H8-H7}$ = 6.7 Hz, H_8), 7.03−6.86 and 6.74−6.63 (m, 4H, H_{26}), 6.87−6.71 (m, 12H, H_{29} H_{33} H_{41} H_{42} H_{43} H_{44}), 6.45 (d, 2H, $^3J_{H32-H33}$ = 8.4 Hz, H_{32}), 6.34 (d, 2H, $^3J_{H1-H2}$ = 8.9 Hz, H_1), 5.58 (t, 2H, $^3J_{H3-H2}$ = $^3J_{H3-H4}$ = 3.5 Hz, H_3), 5.22 (dd, 2H, $^3J_{H2-H1}$ = 8.9 Hz, $^3J_{H2-H3}$ = 3.5 Hz, H_2), 5.11 (dd, 2H, $^3J_{H4-H3}$ = 3.5 Hz, $^3J_{H4-H5}$ = 2.2 Hz, H_4), 4.80 (dd, 2H, $^3J_{H6-H5}$ = 8.6 Hz, $^2J_{H6-H6'}$ = 12.8 Hz, H_6), 4.60−4.54 (m, 2H, H_5), 4.60−4.40 (m, 4H, H_{27}), 4.45 (t, 4H, $^3J_{H17-H16}$ = 7.3 Hz, H_{17}), 4.33−4.25 (m, 2H, $H_{6'}$), 4.22−3.64 (m, 48H, CH_2O), 4.08 (s, 6H, H_{52}), 3.50−3.41 (m, 4H, H_{25}), 3.14−3.07 (br t, 4H, H_{12}), 3.04 (s, 6H, H_{11}), 2.69−2.61 (br t, 4H, H_{20}), 2.20 and 2.16 and 2.02 and 1.90 (4*s, 24H, CH_3CO), 2.00−1.90 (m, 4H, H_{16}), 1.79−1.70 (m, 4H, H_{24}), 1.63−1.50 (m, 4H, H_{13} H_{21}), 1.49−1.35 (m, 8H, H_{14} H_{23}), 1.34−1.25 (m, 4H, H_{15}), 1.22−1.13 (m, 4H, H_{22}); trans isomer δ (ppm) = 8.98 (d, 4H, $^3J_{H7-H8}$ = 6.8 Hz, H_7), 8.09 (s, 2H, H_{18}), 8.07 (d, 4H, $^3J_{H8-H7}$ = 6.1 Hz, H_8), 7.03−6.86 and 6.74−6.63 (m, 4H, H_{26}), 6.87−6.71 (m, 12H, H_{29} H_{33} H_{41} H_{42} H_{43} H_{44}), 6.45 (d, 2H, $^3J_{H32-H33}$ = 8.4 Hz, H_{32}), 6.34 (d, 2H, $^3J_{H1-H2}$ = 8.9 Hz, H_1), 5.58 (t, 2H, $^3J_{H3-H2}$ = $^3J_{H3-H4}$ = 3.5 Hz, H_3), 5.23 (dd, 2H, $^3J_{H2-H1}$ = 8.9 Hz, $^3J_{H2-H3}$ = 3.5 Hz, H_2), 5.11 (dd, 2H, $^3J_{H4-H3}$ = 3.5 Hz, $^3J_{H4-H5}$ = 2.2 Hz, H_4), 4.81 (dd, 2H, $^3J_{H6-H5}$ = 9.0 Hz, $^2J_{H6-H6'}$ = 12.8 Hz, H_6), 4.60−4.54 (m, 2H, H_5), 4.60−4.40 (m, 4H, H_{27}), 4.51 (t, 4H, $^3J_{H17-H16}$ = 7.3 Hz, H_{17}), 4.33−4.25 (m, 2H, $H_{6'}$), 4.22−3.64 (m, 48H, CH_2O), 4.09 (s, 6H, H_{52}), 3.54−3.45 (br t, 4H, H_{12}), 3.50−3.41 (m, 4H, H_{25}), 2.86 (s, 6H, H_{11}), 2.69−2.61 (br t, 4H, H_{20}), 2.20 and 2.16 and 2.01 and 1.90 (4*s, 24H, CH_3CO), 2.00−1.90 (m, 4H, H_{16}), 1.79−1.70 (m, 4H, H_{24}), 1.70−1.63 (m, 4H, H_{13}), 1.63−1.50 (m, 4H, H_{21}), 1.49−1.35 (m, 12H, H_{14} H_{15} H_{23}), 1.22−1.13 (m, 4H, H_{22}). JMOD ^{13}C NMR (100 MHz, CD_3CN, 298 K): δ (ppm) = 171.5 and 170.3 and 170.0 and 170.0 (*C*OCH_3), 165.7 and 165.6 (C_{10}), 156.7 and 156.5 (C_9), 148.7 and 147.1 and 146.9 and 145.5 (C_{19} C_{30} C_{31} C_{32} C_{40} C_{45}), 144.1 and 144.0 (C_7), 128.4 (C_{18}), 127.0 and 126.9 (C_8), 126.2 (C_{28}), 123.5 and 121.6 and 114.1 and 113.0 and 112.7 and 112.7 (C_{29} C_{32} C_{33} C_{41} C_{42} C_{43} C_{44}), 89.1 (C_1), 78.4 and 78.4 (C_5), 72.9 and 72.9 and 71.4 and 71.3 and 71.2 and 71.0 and 68.4 and 68.1 and 68.0 and 67.9 (*C*H_2O), 69.7 and 69.6 (C_2), 68.2 (C_4), 67.5 (C_3), 61.0 and 61.0 (C_6), 54.4 and 54.3 (C_{17}), 52.8 (C_{27}), 51.3 (C_{12cis}), 47.8 ($C_{12trans}$), 49.6 (C_{25}), 38.1 (C_{52}), 37.0 ($C_{11trans}$), 32.7 (C_{11cis}), 29.7 and 29.6 and 28.9 and 28.9 and 28.2 and 27.4 and 27.2 and 26.9 and 26.9 and 26.6 and 26.2 (C_{13} C_{14} C_{15} C_{16} C_{21} C_{22} C_{23} C_{24}), 23.5 (C_{20}), 21.0 and 20.8 and 20.8 and 20.8 and 20.5 and 20.5 (*C*H_3CO). HRMS (ESI): $[M - 4PF_6]^{4+}$ calcd for $[C_{122}H_{178}N_{12}O_{36}\ 2PF_6]^{4+}$ 669.2938, found 669.2930.

2.3. Rotaxane Dimers 4a and 4b. In a typical procedure, Boc_2O (120 mg, 0.550 mmol, 16 equiv) and DIEA (36 mg, 0.275 mmol, 8 equiv) were added to a solution of **1a** (100 mg, 0.0344 mmol, 1 equiv) in 1 mL of dry acetonitrile. After 62 h at rt, the solvent was evaporated, and the mixture was dissolved in 10 mL of dichloromethane. The organic layer was washed twice with 10 mL of an aqueous solution of HCl 1 M and twice with 10 mL of a $NaHCO_3$ saturated aqueous solution. The aqueous layers were extracted with dichloromethane, and the combined organics layers were dried over $MgSO_4$ and concentrated. The obtained solid was washed with diethyl ether and purified by chromatography on a Sephadex LH20 column (eluent CH_2Cl_2/MeOH 1:1) to give the desired product **4a** (68 mg, 70%) as a yellow solid.

a. The rotaxane dimer **4a** (R = H) was obtained in 70% yield after 62 h of reaction R_f (CH_2Cl_2/MeOH 9:1): 0.59. ^{1}H NMR (400 MHz, CD_3CN, 298 K): δ (ppm) = 9.35 (d, 4H, $^3J_{H8-H7}$ = 6.4 Hz, H_8), 8.99 (d, 4H, $^3J_{H7-H8}$ = 6.4 Hz, H_7), 7.96−7.88 (br t, 2H, H_{11}), 7.49 (s, 2H, H_{18}), 7.04−6.79 (m, 14H, H_{29} H_{32} H_{33} H_{41} H_{42} H_{43} H_{44}), 6.34 (d, 2H, $^3J_{H1-H2}$ = 9.2 Hz, H_1), 5.45 (t, 2H, $^3J_{H3-H2}$ = $^3J_{H3-H4}$ = 3.5 Hz, H_3), 5.27 (dd, 2H, $^3J_{H2-H1}$ = 9.2 Hz, $^3J_{H2-H3}$ = 3.5 Hz, H_2), 5.00 (dd, 2H, $^3J_{H4-H3}$ = 3.5 Hz, $^3J_{H4-H5}$ = 1.6 Hz, H_4), 5.02−4.92 (m, 2H, H_6), 4.40−4.25 (m, 6H, H_5 H_{27}), 4.21 (t, 4H, $^3J_{H17-H16}$ = 7.0 Hz, H_{17}), 4.17−3.99 (m, 18H, $H_{6'}$ H_{34} H_{39} H_{46} H_{51}), 3.80−3.50 (m, 20H, CH_2O), 3.25−2.96 (m, 20H, H_{12} H_{25} CH_2O), 2.61 (t, 4H, $^3J_{H20-H21}$ = 7.3 Hz, H_{20}), 2.16 and 2.12 and 2.00 and 1.84 (4*s, 24H, CH_3CO), 1.73−1.64 (m, 4H, H_{16}), 1.63−1.53 (m, 4H, H_{21}), 1.44 (s, 18H, H_{26}), 1.49−1.37 (m, 4H, H_{24}),1.36−1.18 (m, 8H, H_{22} H_{23}), 1.16−1.01 (m, 12H, H_{13} H_{14} H_{15}). JMOD ^{13}C NMR (100 MHz, CD_3CN, 298 K): δ (ppm) = 171.7 and 170.2 and 170.0 and 169.8 (*C*OCH_3), 163.0 (C_{10}), 152.3 and 148.7 and 148.6 and 148.5 and 148.4 and 147.6 (C_9 C_{19} C_{30} C_{31} C_{40} C_{45} N*C*OO), 142.8 (C_7), 133.2 (C_{28}), 130.2 (C_8), 122.5 and 122.3 and 122.1 and 121.1 and 112.8 and 112.7 and 112.5 and 112.5 (C_{29} C_{32} C_{33} C_{41} C_{42} C_{43} C_{44}), 88.6 (C_1), 79.9 (C_5), 79.0 (*C*$(CH_3)_3$), 71.3 and 71.0 and 70.5 and 70.3 and 70.1 and 69.7 and 69.6 and 69.3 and 69.2 and 69.1 and 69.0 (*C*H_2O), 68.8 (C_2), 68.2 (C_4), 67.3 (C_3), 60.3 (C_6), 50.5 (C_{17}), 50.4 (C_{27}), 47.3 (C_{25}), 40.6 (C_{12}), 30.7 and 30.1 and 29.4 and 29.4 and 27.2 and 26.5 (C_{13} C_{14} C_{15} C_{16} C_{21} C_{22} C_{23} C_{24}), 26.0 (C_{20}), 27.4 ((*C*$H_3)_3$C), 21.0 and 20.9 and 20.8 and 20.7 (*C*H_3CO). HRMS (ESI): $[M - 2PF_6 + 2H]^{4+}$ calcd for $[C_{128}\ H_{184}N_{12}O_{40}]^{4+}$ 632.3150, found 632.3179.

b. The rotaxane dimer **4b** (R = Me) was obtained in 75% yield after 16 days of reaction. R_f (CH_2Cl_2/MeOH 9:1): 0.59. Ratio of isomers *cis*/*trans* 47:53. ^{1}H NMR (400 MHz, CD_3CN, 298 K): cis isomer δ (ppm) = 9.92−9.82 (br s, 4H, H_7), 8.01 (d, 4H, $^3J_{H8-H7}$ = 5.7 Hz, H_8), 7.45 (s, 2H, H_{18}), 7.10−6.70 (m, 14H, H_{29} H_{32} H_{33} H_{41} H_{42} H_{43} H_{44}), 6.35 (s, 2H, H_1), 5.90 (br s, 2H, H_2), 5.50−5.38 (m, 2H, H_3), 5.17 (t, 2H, $^3J_{H4-H3}$ = $^3J_{H4-H5}$ = 8.0 Hz, H_4), 4.39−4.20 (m, 6H, H_5 H_{17}), 4.20−4.07 (m, 4H, H_6 $H_{6'}$), 4.39−3.83 (m, 20H, H_{27} H_{34} H_{39} H_{46} H_{51}), 3.81−3.51 (m, 16H, H_{35} H_{38} H_{47} H_{50}), 3.51−3.33 and 3.21−3.02 (m, 16H, H_{36} H_{37} H_{48} H_{49}), 3.21−3.02 (m, 8H, H_{12} H_{25}), 3.01 (s, 6H, H_{11}), 2.65−2.53 (m, 4H, H_{20}), 2.12 and 1.81 and 1.78 and 1.76 (4*s, 24H, CH_3CO), 1.88−1.73 (m, 4H, H_{16}), 1.43 (s, 18H, H_{26}), 1.63−1.05 (m, 28H, H_{13} H_{14} H_{15} H_{21} H_{22} H_{23} H_{24}); trans isomer δ (ppm) = 9.95 (d, 4H, $^3J_{H7-H8}$ = 5.8 Hz, H_7), 8.05 (d, 4H, $^3J_{H8-H7}$ = 5.8 Hz, H_8), 7.48 (s, 2H, H_{18}), 7.15−6.70 (m, 14H, H_{29} H_{32} H_{33} H_{41} H_{42} H_{43} H_{44}), 6.35 (s, 2H, H_1), 5.95 (br s, 2H, H_2), 5.50−5.38 (m, 2H, H_3), 5.17 (t, 2H, $^3J_{H4-H3}$ = $^3J_{H4-H5}$ = 8.0 Hz, H_4), 4.39−4.20 (m, 6H, H_5 H_{17}), 4.20−4.07 (m, 4H, H_6 $H_{6'}$), 4.39−3.83 (m, 20H, H_{27} H_{34} H_{39} H_{46} H_{51}), 3.81−3.51 (m, 16H, H_{35} H_{38} H_{47} H_{50}), 3.51−3.33 and 3.21−3.02 (m, 16H, H_{36} H_{37} H_{48} H_{49}), 3.51−3.33 (m, 4H, H_{12}), 3.21−3.02 (m, 4H, H_{25}), 2.82 (s, 6H, H_{11}), 2.65−2.53 (m, 4H, H_{20}), 2.12 and 1.81 and 1.78 and 1.76 (4*s, 24H, CH_3CO), 1.88−1.73 (m, 4H, H_{16}), 1.43 (s, 18H, H_{26}), 1.63−1.05 (m, 28H, H_{13} H_{14} H_{15} H_{21} H_{22} H_{23} H_{24}). JMOD ^{13}C NMR (100 MHz, CD_3CN, 298 K): δ (ppm) = 171.0 and 170.3 and 169.9 and 169.8 and 169.7 (*C*OCH_3), 166.8 (C_{10}), 153.6 and 153.3 (C_9), 148.5 and 148.4 and 148.1 and 147.5 (C_{19} C_{30} C_{31} C_{40} C_{45} N*C*OO), 147.7 (C_7), 133.0 (C_{28}), 125.6 and 125.0 (C_8), 122.0 (C_{18}), 122.2 and 121.0 and 113.3 and 113.2 and 113.0 and 112.9 (C_{29} C_{32} C_{33} C_{41} C_{42} C_{43} C_{44}), 93.4 and 92.9 (C_1), 79.9 (C_5), 72.7 and 72.5 and 71.3 and 71.2 and 69.4 and 69.3 and 69.2 (*C*H_2O), 68.8 (C_2), 68.8 (C_3), 66.5 (C_4), 61.6 (C_6), 51.5 (C_{12cis}), 47.4 ($C_{12trans}$), 50.4 and 50.3

(C_{17}), 50.3 (C_{27}), 47.4 (C_{25}), 37.1 ($C_{11trans}$), 32.6 (C_{11cis}), 30.7 (C_{16}), 30.2 and 30.1 and 29.5 and 29.4 27.2 and 27.1 and 27.0 and 26.8 and 26.7 and 26.6 (C_{13} C_{14} C_{15} C_{21} C_{22} C_{23} C_{24}), 28.6 (C_{26}), 26.1 and 26.0 (C_{20}), 20.8 and 20.6 (CH_3CO). HRMS (ESI): $[M - 2PF_6 + 2H]^{4+}$ calcd for $[C_{130}H_{188}N_{12}O_{40}]^{4+}$ 639.3262, found 639.3235.

2.4. Rotaxane dimer 5a. The rotaxane dimer **5a** was obtained in 96% yield from **4a** using the typical methylation procedure described in section 2.2.

R_f (CH_2Cl_2/MeOH 9:1): 0.33. ^{1}H NMR (400 MHz, CD_3CN, 298 K): δ (ppm) = 9.02 (d, 4H, $^3J_{H7-H8}$ = 6.9 Hz, H_7), 8.75−8.63 (br s, 4H, H_8), 8.55−8.44 (br s, 2H, H_{18}), 7.79−7.72 (br t, 2H, H_{11}), 6.94−6.66 (m, 14H, H_{29} H_{32} H_{33} H_{41} H_{42} H_{43} H_{44}), 6.37 (d, 2H, $^3J_{H1-H2}$ = 9.1 Hz, H_1), 5.53 (t, 2H, $^3J_{H3-H2}$ = $^3J_{H3-H4}$ = 3.4 Hz, H_3), 5.24 (dd, 2H, $^3J_{H2-H1}$ = 9.1 Hz, $^3J_{H2-H3}$ = 3.4 Hz, H_2), 5.08 (dd, 2H, $^3J_{H4-H3}$ = 3.4 Hz, $^3J_{H4-H5}$ = 1.9 Hz, H_4), 4.88 (dd, 2H, $^3J_{H6-H5}$ = 9.5 Hz, $^2J_{H6-H6'}$ = 12.8 Hz, H_6), 4.81−4.68 (br s, 4H, H_{17}), 4.53−4.47 (m, 2H, H_5), 4.35−4.17 (m, 4H, H_{27}), 4.21 (dd, 2H, $^3J_{H6'-H5}$ = 3.4 Hz, $^2J_{H6'-H6}$ = 12.8 Hz, $H_{6'}$), 4.34−3.93 (m, 16H, H_{34} H_{39} H_{46} H_{51}), 4.83−3.58 (m, 16H, H_{35} H_{38} H_{47} H_{50}), 3.75 (s, 6H, H_{52}), 3.50−3.14 (m, 24H, H_{12} H_{25} H_{36} H_{37} H_{48} H_{49}), 3.14−3.03 (br s, 4H, H_{20}), 2.18 and 2.11 and 1.99 and 1.86 (4*s, 24H, CH_3CO), 2.12−2.00 (m, 4H, H_{16}), 1.56−1.37 (m, 12H, H_{13} H_{21} H_{24}), 1.43 (s, 18H, H_{26}), 1.36−1.10 (m, 16H, H_{14} H_{15} H_{22} H_{23}). JMOD ^{13}C NMR (100 MHz, CD_3CN, 298 K): δ (ppm) = 171.7 and 170.3 and 170.0 and 169.9 ($COCH_3$), 162.6 (C_{10}), 152.8 (C_9), 148.7 and 148.6 and 148.5 and 147.7 (C_{19} C_{30} C_{31} C_{40} C_{45} $NCOO$), 143.7 (C_7), 132.6 (C_{28}), 128.3 (C_8), 121.8 and 112.7 and 112.5 and 111.9 (C_{29} C_{32} C_{33} C_{41} C_{42} C_{43} C_{44}), 88.9 (C_1), 80.0 ($C(CH_3)_3$), 78.8 (C_5), 71.4 and 71.2 and 70.7 and 70.5 and 69.1 and 69.0 and 68.9 (CH_2O), 69.4 (C_2), 68.2 (C_4), 67.4 (C_3), 60.7 (C_6), 54.3 (C_{17}), 50.0 (C_{25}), 49.1 (C_{27}), 40.8 (C_{12}), 37.3 (C_{52}), 29.5 and 27.0 and 26.5 (C_{13} C_{14} C_{15} C_{16} C_{21} C_{22} C_{23} C_{24}), 28.7 (C_{26}), 23.4 (C_{20}), 21.0 and 20.9 and 20.8 and 20.6 (CH_3CO). HRMS (ESI): $[M - 4PF_6]^{4+}$ calcd for $[C_{130}H_{188}N_{12}O_{40}]^{4+}$ 639.3262, found 639.3242.

2.5. Rotaxane Dimer 5b. The rotaxane dimer **5b** was obtained in 91% yield from **4b** using the typical methylation procedure described in section 2.2. It could be as well obtained in a 73% yield from **2b** after 5 days using the typical carbamoylation procedure described in section 2.3. R_f (CH_2Cl_2/MeOH 9:1): 0.64. Ratio of isomers *cis*/*trans* 42:58. ^{1}H NMR (400 MHz, CD_3CN, 298 K): cis isomer δ (ppm) = 9.01 (d, 4H, $^3J_{H7-H8}$ = 6.7 Hz, H_7), 8.77−8.57 (br s, 2H, H_{18}), 8.03 (d, 4H, $^3J_{H8-H7}$ = 6.7 Hz, H_8), 6.98−6.64 (m, 14H, H_{29} H_{32} H_{33} H_{41} H_{42} H_{43} H_{44}), 6.42 (d, 2H, $^3J_{H1-H2}$ = 8.8 Hz, H_1), 5.57 (t, 2H, $^3J_{H3-H2}$ = $^3J_{H3-H4}$ = 3.5 Hz, H_3), 5.21 (dd, 2H, $^3J_{H2-H1}$ = 8.8 Hz, $^3J_{H2-H3}$ = 3.5 Hz, H_2), 5.12 (dd, 2H, $^3J_{H4-H3}$ = 3.5 Hz, $^3J_{H4-H5}$ = 2.2 Hz, H_4), 5.06−4.86 (br s, 4H, H_{17}), 4.82 (dd, 2H, $^3J_{H6-H5}$ = 8.8 Hz, $^2J_{H6-H6'}$ = 12.8 Hz, H_6), 4.60−4.53 (m, 2H, H_5), 4.33−4.25 (m, 2H, $H_{6'}$), 4.33−4.16 (m, 4H, H_{27}), 4.15−3.89 (m, 16H, H_{34} H_{39} H_{46} H_{51}), 3.87−3.71 (m, 16H, H_{35} H_{38} H_{47} H_{50}), 3.71−3.46 (m, 16H, H_{36} H_{37} H_{48} H_{49}), 3.67 (s, 6H, H_{52}), 3.19−3.04 (m, 4H, H_{25}), 3.06−2.96 (br t, 4H, H_{12}), 3.00 (s, 6H, H_{11}), 2.79−2.68 (m, 4H, H_{20}), 2.21 and 2.12 and 1.99 and 1.88 (4*s, 24H, CH_3CO), 2.00−1.90 (m, 4H, H_{16}), 1.69−1.55 (m, 8H, H_{13} H_{21}), 1.43 (s, 18H, H_{26}), 1.54−1.09 (m, H_{14} H_{15} H_{22} H_{23} H_{24}); trans isomer δ (ppm) = 9.01 (d, 4H, $^3J_{H7-H8}$ = 6.7 Hz, H_7), 8.77−8.57 (br s, 2H, H_{18}), 8.05 (d, 4H, $^3J_{H8-H7}$ = 6.7 Hz, H_8), 6.98−6.64 (m, 14H, H_{29} H_{32} H_{33} H_{41} H_{42} H_{43} H_{44}), 6.40 (d, 2H, $^3J_{H1-H2}$ = 8.8 Hz, H_1), 5.57 (t, 2H, $^3J_{H3-H2}$ = $^3J_{H3-H4}$ = 3.5 Hz, H_3), 5.23 (dd, 2H, $^3J_{H2-H1}$ = 8.8 Hz, $^3J_{H2-H3}$ = 3.5 Hz, H_2), 5.12 (dd, 2H, $^3J_{H4-H3}$ = 3.5 Hz, $^3J_{H4-H5}$ = 2.2 Hz, H_4), 5.06−4.86 (br s, 4H, H_{17}), 4.81 (dd, 2H, $^3J_{H6-H5}$ = 9.0 Hz, $^2J_{H6-H6'}$ = 12.8 Hz, H_6), 4.60−4.53 (m, 2H, H_5), 4.33−4.25 (m, 2H, $H_{6'}$), 4.33−4.16 (m, 4H, H_{27}), 4.15−3.89 (m, 16H, H_{34} H_{39} H_{46} H_{51}), 3.87−3.71 (m, 16H, H_{35} H_{38} H_{47} H_{50}), 3.71−3.46 (m, 16H, H_{36} H_{37} H_{48} H_{49}), 3.67 (s, 6H, H_{52}), 3.46−3.39 (br t, 4H, H_{12}), 3.19−3.04 (m, 4H, H_{25}), 2.82 (s, 6H, H_{11}), 2.79−2.68 (m, 4H, H_{20}), 2.21 and 2.16 and 2.01 and 1.90 (4*s, 24H, CH_3CO), 2.00−1.90 (m, 4H, H_{16}), 1.69−1.56 (m, 8H, H_{13} H_{21}), 1.43 (s, 18H, H_{26}), 1.54−1.09 (m, H_{14} H_{15} H_{22} H_{23} H_{24}). JMOD ^{13}C NMR (100 MHz, CD_3CN, 298 K): δ (ppm) = 171.5 and 171.5 and 170.3 and 170.1 and 170.0 ($COCH_3$), 165.7 and 165.5 (C_{10}), 156.7 and 156.5 (C_9), 148.7 and 148.7 and 148.6 and 148.6 and 148.5 and 148.4 and 147.7 (C_{19} C_{30} C_{31} C_{32} C_{40} C_{45} $NCOO$), 144.1 (C_7), 132.4 (C_{28}), 129.4 (C_{18}), 127.0 and 126.9 (C_8), 122.4 and 122.3 and 121.6 and 115.1 and 112.5 and 111.9 (C_{29} C_{32} C_{33} C_{41} C_{42} C_{43} C_{44}), 89.1 and 89.0 (C_1), 80.0 ($C(CH_3)_3$), 78.5 and 78.5 (C_5), 71.9 and 71.7 and 71.2 and 70.8 and 70.6 and 70.3 and 70.2 and 69.8 and 69.4 and 69.1 and 69.0 and 68.9 (CH_2O), 69.7 and 69.6 (C_2), 68.2 (C_4), 67.5 (C_3), 61.1 (C_6), 54.3 and 54.2 (C_{17}), 51.4 (C_{12cis}) 48.0 ($C_{12trans}$), 50.0 (C_{27}), 47.0 (C_{25}), 38.1 (C_{52}), 37.1($C_{11trans}$), 32.8 (C_{11cis}), 28.7 ($C(CH_3)_3$), 27.4 and 27.3 and 27.0 and 26.9 and 26.9 and 26.2 and 23.6 and 23.6 and 23.3 (C_{13} C_{14} C_{15} C_{16} C_{21} C_{22} C_{23} C_{24}), 23.2 (C_{20}), 21.0 and 20.9 and 20.8 and 20.6 and 20.5 (CH_3CO).

2.6. Reprotonation Procedure of Rotaxane Dimers 4a,b and 5a, b. In a typical procedure, the rotaxane dimer **4a** (12 mg, $4.26.10^{-6}$ mol) was suspended in 1 mL of a solution of HCl (2 M) in diethyl ether and stirred for 30 min at room temperature. After evaporation, the solid was washed with diethyl ether. Then, NH_4PF_6 (3.5 mg, $2.130.10^{-5}$ mol, 5 equiv) and 1 mL of dichloromethane were added to a suspension of the previous product in 1 mL of Milli-Q water. The resulted bilayer solution was vigorously stirred for 30 min. After separation, the aqueous layer was extracted with 5 mL of dichloromethane. The organic layers were combined, dried over $MgSO_4$, and concentrated to obtain the rotaxane dimer **1a** (11 mg, 89%) as a yellow solid.

Acknowledgment. This research was supported by the Ligue National Contre le Cancer (LNCC). We thank Professor Jean Martinez (Director of the Institut des Biomolécules Max Mousseron) for his help in finding Doctoral Fellowship and for support.

Supporting Information Available: Characterization data with full experimental procedures for starting materials, monomers, and [c2]daisy chains. This material is available free of charge via the Internet at http://pubs.acs.org.